ROLE OF P53 IN ADAPTATION TO THE TUMOR MICROENVIRONMENT

by

Erin E. Mendoza

_____

A Dissertation Submitted to the Faculty of the

DEPARTMENT OF NUTRITIONAL SCIENCES

In Partial Fulfillment of the Requirements
For the Degree of

DOCTOR OF PHILOSOPHY

In the Graduate College

THE UNIVERSITY OF ARIZONA

2010

THE UNIVERSITY OF ARIZONA
GRADUATE COLLEGE

As members of the Dissertation Committee, we certify that we have read the dissertation prepared by Erin E. Mendoza , entitled “Role of p53 in Adaptation to the Tumor Microenvironment” and recommend that it be accepted as fulfilling the dissertation requirement for the Degree of Doctor of Philosophy

_____Date: 4/23/10
Kirsten H. Limesand, Ph.D.

_____Date: 4/23/10
Donato F. Romagnolo, Ph.D.

_____Date: 4/23/10
Amanda F. Baker, Pharm.D., Ph.D.

_____Date: 4/23/10
Vince Guerriero, Ph.D.

Final approval and acceptance of this dissertation is contingent upon the candidate's submission of the final copies of the dissertation to the Graduate College.

I hereby certify that I have read this dissertation prepared under my direction and recommend that it be accepted as fulfilling the dissertation requirement.

_____Date: 4/23/10
Dissertation Director: Randy Burd, Ph.D.

STATEMENT BY AUTHOR

This dissertation has been submitted in partial fulfillment of requirements for an advanced degree at the University of Arizona and is deposited in the University Library to be made available to borrowers under rules of the Library.

Brief quotations from this dissertation are allowable without special permission, provided that accurate acknowledgment of source is made. Requests for permission for extended quotation from or reproduction of this manuscript in whole or in part may be granted by the head of the major department or the Dean of the Graduate College when in his or her judgment the proposed use of the material is in the interests of scholarship. In all other instances, however, permission must be obtained from the author.

SIGNED: Erin E. Mendoza

TABLE OF CONTENTS

TABLE OF CONTENTS - *Continued*

TABLE OF CONTENTS - *Continued*

TABLE OF CONTENTS - *Continued*

TABLE OF CONTENTS - *Continued*

LIST OF FIGURES

Page

LIST OF FIGURES - *Continued*

LIST OF TABLES

Page

ABSTRACT

Tumors cells grow in nutrient and oxygen-deprived microenvironments and adapt to the suboptimal growth conditions by altering their metabolic pathways. The adaptation process commonly creates a tumor phenotype of high glycolytic potential and aggressive growth characteristics which facilitate metastasis and confer resistance to radiation and chemotherapy. Understanding the mechanisms that allow tumors to adapt and survive in their microenvironment is crucial to cancer prevention and control. It was hypothesized that the tumor microenvironment would induce signaling and enzymatic changes, which if manipulated could improve treatment outcome. The results presented here demonstrate that exposure of tumor cells to chronic low pH or hypoxic conditions induced signaling cascades and altered enzyme profiles which resulted in a pro-survival phenotype. Three key adaptation events were observed and included **1)** the up regulation of the metabolic stress and glycolytic proteins AMP-activated protein kinase (AMPK) and 6-Phosphofructo-2-Kinase/Fructose-2,6-Biphosphatase 3 (PFKFB3), respectfully. **2)** The upregulation of p53 and **3)** changes in the ratios of the bioreductive enzymes were also found to be important in the adaptation. The tumor suppressor p53 played a central role in adaptation because it induced the transcription of anti-glycolytic proteins to control glycolysis and minimize tumor cell acidosis. The ratio of bioreductive enzymes was also altered by changes to the microenvironment. Hypoxia had the greatest effect on protein levels and caused a decrease in the ratio of NAD(P)H:quinone oxidoreductase 1 (NQO1): cytochrome p450 reductase. The increase in cytochrome p450 reductase, a one electron bioreduction enzyme, has been shown to increase toxicity of

bioreductive drugs in hypoxic tumors. Micronutrients also had an effect on p53 homeostasis because increasing NQO1 activity by riboflavin supplementation induced a p53-stabilizing effect by enhancing binding of p53 to NQO1, protecting the tumor suppressor from degradation. Taken together, these results indicate the changes that occur in tumor adaptation to the microenvironment require signaling and enzymatic changes that work in concert to regulate metabolism and apoptosis. Many of these changes present therapeutic targets that could be exploited to enhance therapy or prevent adaptation and subsequent tumor growth.

CHAPTER I: INTRODUCTION

Overview

Tumors are highly metabolic tissues that require a high rate of blood perfusion for nutrient delivery and removal of metabolites. The high demand for perfusion results in the secretion of cytokines by the tumors which promote vasculaturization of the tumor and tumor bed (Wachsberger et. al., 2007). However, the neovasculature that forms is tortuous and inefficient and results in poor perfusion. The diffusion of oxygen is limited, and therefore glucose, which has a greater diffusion distance, can penetrate the tumor (Fang et. al., 2008). In the absence of oxygen in perfusion limited areas, glucose becomes the preferred energy-bearing nutrient and is ultimately converted into lactic acid. The combination of poor oxygen delivery and the subsequent generation of ATP through acid producing glycolysis creates an hypoxic and acidic microenvironment. This hostile tumor environment selects for aggressive tumor characteristics that affect the growth of the tumor, promote its invasive nature, and increases the risk of metastasis (Semenza, 2009). Moreover, these genetic and molecular changes that result produce a tumor phenotype that is resistant to radiation and chemotherapy (Semenza, 2008). Understanding the factors and mechanisms that allow a tumor to adapt and survive in the

tumor microenvironment is crucial to tumor prevention and control. Therefore it is the overall goal of this dissertation to test the hypothesis that the tumor microenvironment will induce signaling and enzymatic changes, which if manipulated can improve prevention or treatment outcome. This dissertation will test the 3 subhypotheses that 1) the acid microenvironment will induce signaling cascades and enzymatic changes to promote to tumor cell survival; 2) Nutrients and co-factors in the tumor microenvironment can affect tumor survival and produce pro-tumorigenic conditions; 3) The acidic and enzymatic properties be manipulated to prevent or control tumors.

Tumor Hypoxia and Hif-1

Hypoxia is a physiological condition characterized by low oxygen tension that occurs in several pathological states. Hypoxia can be chronic or acute depending on the situation (Semenza, 2008). In chronic hypoxia adaptation to a change in oxygen tension must occur to avoid a disruption in energy production and consumption. The central mediator of hypoxic signaling is hypoxia inducible factor 1 (Hif-1) which is upregulated in response to a drop in tissue oxygen levels and leads to a cascade of microenvironmental changes that ultimately lead to tumor adaptation and changes in the genetic profile of the tumor leading to cell survival (Rekwirowicz and Marszalek, 2009).

Hif-1 is a heterodimeric protein composed of an oxygen sensitive alpha subunit and constitutively active beta subunit. Downstream target genes have a hypoxia responsive element (HRE), and 1 to 2% of the human genome possesses the HRE. Hypoxia signaling mediated by Hif-1 is dependent upon post-translational hydroxylation of proline residues catalyzed by oxygen sensing dioxegenases referred to as Hif hydroxylases. One type of Hif hydroxylase, HIF-prolyl hydroxylases also referred to as prolyl hydroxylase domain (PHD), proteins hydroxylate two proline residues on the alpha subunit. These PHD proteins are strictly regegulated by oxygen tension and these two residues are located in the oxygen- dependent degradation (ODD) domain of HIFα and when hydroxylated this domain has strong affinity for the von Hippel-Lindau (VHL) protein, a component of an E3 ubiquitin ligase complex (Semenza, 2009). The consequence is poly-ubiq- uitination and targeting of Hif-1 for degradation by the proteasome. Thus an increase in Hif-1 protein levels in hypoxia is due to the inhibition of this oxygen-dependent degradation process (Koh et. al., 2010; Poon et. al., 2009; Rekwirowicz and Marszalek, 2009; Semenza, 2008).

Mechanisms of tumor angiogenesis

The formation of new blood vessels in solid tumors serves to provide blood, oxygen, and nutrients to promote further growth. Angiogenesis is not limited to only tumors but is also seen in other physiological and pathological states (Ferrara et. al., 2003). It has been observed that the formation of new blood vessels and the commencement angiogenesis during the hyperplastic or dysplastic phases can lead to tumorigenesis, progression of the tumor, and finally metastasis (Jain, 2005). Angiogenesis occurs as a result of an imbalance between pro- and antiangiogenic factors (Nieder et. al., 2006). There have been many angiogenic factors identified such as vascular endothelial growth factor (VEGF), fibroblast growth factor (FGF), platelet-derived growth factor (PDGF), transforming growth factor beta-1 (TGF-β1), and epidermal growth factor (EGF) (Ferrara et. al., 2003; McMahon, 2000; Nieder et. al., 2006). Endogenous anti-angiogenic growth factors have also been identified such as endostatin and angiostatin (Nieder et. al., 2006). The most widely studied and best characterized angiogenic factor is VEGF. VEGF is the most potent of the growth factors eliciting the most pronounced affect on neovascularization (McMahon, 2000). There have been six members of the VEGF family belonging to the PDGF superfamily identified:

VEGF, VEGF-B, VEGF-C, VEGF-D, VEGF-E, and placenta growth factor. All members of the VEGF family are dimeric glycoproteins. VEGF is expressed is the majority of solid tumors and survival of newly formed endothelial cells is dependent upon levels of VEGF (Inai et. al., 2004; McMahon, 2000). VEGF is also referred to as vascular permeability factor because of its ability to cause the vasculature to become dilated and leaky. The most striking biological feature of VEGF in vivo is its ability to cause rapid vasculature leakage upon injection (Dvorak, 2002). The proposed sequence of steps of new vessel formation is the onset of hyperpermeability in the vessels resulting in tissue edema. The formation of "mother vessels" are characteristically thin walled and poor in pericytes, and function in stabilizing the endothelial wall of the vessel. These vessels form as a result of basement membrane degradation, detachment of pericytes from the residual basement membrane, followed by expansion of the remaining endothelium to cover the area were the basement membrane existed (Dvorak, 2002).

Mediation of VEGF occurs through two transmembrane receptor tyrosine kinases VEGFR-1 and VEGFR-2, which are overexpressed in tumors showing overexpression of VEGF (Dvorak, 2002; Ferrara et. al., 2003). After binding to its receptors, VEGF begins a sequence of signal events that lead to the activation of several downstream signaling

pathways such as mitogen-activated protein kinase (MAPK) and phosphatidylinositol 3-kinase (Dvorak, 2002). The cascade begins with receptor dimerization upon ligand binding and autophosphorylation of tyrosine residues (McMahon, 2000). Although definitive functions of the receptors has not been clearly established, it is accepted that the high-affinity VEGFR-2 is found only in endothelial cells (McMahon, 2000) and serves as a mediator for the permeability inducing affects of VEGF followed by proliferation and migration of endothelial cells marking the angiogenic effects of VEGF (Dvorak, 2002; Ferrara et. al., 2003; Tozer and Bicknell, 2004). Hypoxic conditions serve as a potent activator for the transcription and stabilization of VEGF (Dvorak, 2002). Transcription of HIF-1 as a hypoxic response is a powerful stimulus for induction of VEGF expression (Jain, 2003). In oxic conditions, HIF-1α is rapidly degraded (Jain, 2003) whereas in a hypoxic tumor microenvironment, HIF-1α is stabilized and subsequently dimerizes with HIF-1β and the complex in turn binds to the VEGF promoter, activating transcription (Dvorak, 2002). It has also been shown that HIF-1α expression as a result of hypoxia upregulates the expression of VEGFR-1 (Ferrara et. al., 2003).

Radiation therapy and the importance of oxygen

Radiation therapy is used in the treatment of several tumor types and the number of patients undergoing radiation therapy is rapidly growing (Owen et. al., 1992). Radiation sterilizes or kills tumor cells by inducing the formation of free radical species (Poon et. al., 2009) that damage the DNA of the cells (Hall, 2000). Repair of damage is severely inhibited by the presence of oxygen at the site of irradiation and tumor cells can be sensitized up to 3 fold by the presence of oxygen (Chan et. al., 2009). Because many tumors are hypoxic, the full potential of radiation therapy is not realized. Elucidation of the mechanisms involved in tumorigenesis reveal that the induction of angiogenesis as a major factor promoting tumor growth and tumor hypoxia (Fukumura and Jain, 2007). It has also been observed that radiation can induce angiogenic factors that may contribute to hypoxia or radiation resistance. Angiogenesis can promote an inefficient vascular supply in tumors and result in tumor hypoxia (Jain, 2001). One approach to treating hypoxic tumors is to eliminate the neovasculature and restore blood flow. This can be accomplished by the use of anti-angiogenic drugs. A common quest in preclinical studies that use anti-angiogenic compounds is to induce “normalization” of tumor vascular, or a therapeutic window of increased oxygen tension (Wachsberger, 2007). The

normalization would increase or normalize tumor perfusion and induce oxygenation of the tumor. Although normalization may be temporary and dependent on drug scheduling, the temporary oxygenation provides a "window of opportunity" where radiation would theoretically be more effective.

The seemingly counterintuitive hypothesis that by destroying emerging tumor vascular via antiangiogenic therapy will improve oxygen perfusion and ultimately improve radiation and chemotherapy outcomes is becoming more widely accepted. The notion of normalization of the vascular entails a marked decrease in the immature blood vessels that are inefficient in their nutrient delivery to the tumor and contribute significantly to the hypoxia characteristic of the tumor microenvironment (Jain, 2005). The nature of the tumor vessels is the target for the concept of normalization. In a growing tumor, angiogenic factors are recruited to promote the formation of new blood vessels, which in theory should improve growth by means of increasing nutrient delivery and oxygen flow to the tumor. The newly formed blood vessels have abnormal morphology in that they have loosely attaching pericytes, basement membrane abnormalities, varying in diameter, and are leaky in nature leading to an increased interstitial fluid pressure (Inai et. al., 2004; Tong et. al., 2004). The destruction of these

unstable vessels through antiangiogenic therapy promotes the further recruitment of pericytes that act in stabilizing the remaining vessels in the tumor (Jain, 2005). The resulting normalization serves as a window for optimal application of radiation therapy. The novel mechanism of the "normalization window" is crucial to maximizing the delivery of radiation or chemotherapy and still is not known and is under current investigation.

Therapies to Normalize Vasculature

It is hypothesized that uncontrolled VEGF signaling is a key contributor to the atypical architecture of the vasculature (Wachsberger, 2007). It has been observed that interfering with VEGF signaling results in regression of the tortuous vessels resulting in normalization. Pruning the less efficient vasculature with antiangiogenics allows the remaining vasculature to be used for delivery of oxygen, nutrients, as well as chemotherapeutics. Winkler et. al. (2004) investigated the time course associated with the application of radiation therapy following treatment with the monoclonal antibody against VEGFR2, DC101, in human U87 glioma xenographs. The resulting alterations in tumor oxygen perfusion and radiation response were explored. A combination of DC101 and γ radiation along with monotherapy of each was applied to tumors in varying time

frames. Following monotherapy of DC101, an insignificant delay in tumor growth was observed. Radiation therapy alone applied in three daily fractionated doses showed significant delay in tumor growth. Radiation applied in combination with DC101 showed an optimal application window at days 4-6 delaying tumor growth significantly indicating a synergistic effect. After further review, it was observed that the days that showed the greatest delay in tumor growth paralleled a decrease in hypoxia levels in the tumors. On day 2, the oxygen perfusion in the tumor was greatly increased and hypoxia was nearly nonexistent by day 5, increasing again by day 8. These results raise the question on what is ameliorating the oxygen perfusion in the tumors. The results implicated the mechanism of the assumed normalization of the vasculature resulted in diminished hypoxia due in part to the increased migration of pericytes to the vessels stabilizing them (Winkler et. al., 2004). Tong et al showed that treatment with DC101 in MCaIV murine mammary carcinoma showed a remarkable reduction of vessel tortuosity after 2-3 days and the vessels took on a more normal morphology. By day 5 of treatment, some regions of the tumor showed complete regression, indicating that normalization occurs before vessel regression. The treatment with DC101 also demonstrated normalization of the wall

structure of the tumor vasculature. After treatment only 8% of the cells showed slight perivascular coverage, compared with 25% in the untreated cells (Tong et. al., 2004).

The induction of VEGF upon application of ionizing radiation gives significant cause to the importance of regulation of angiogenic factors. The upregulation of proangiogenic cytokines ultimately leads to radiation resistant tumors that have shown clinically a poorer prognosis (Huber et. al., 2005). The dogma for the combination of antiangiogenic therapy and ionizing radiation is to destroy tumor endothelial cells while suppressing further regeneration of the tumor vasculature. Gorski et. al. (1999) showed that Lewis Lung Carcinoma displayed a dose-dependent increase in the expression of VEGF following ionizing radiation. Combined treatment with anti-VEGF antibodies significantly reduced tumor doubling time (Gorski et. al., 1999). A concern with treatments that target specific angiogenic factors is the possibly of tumors developing resistance. A possible alternative is to developing a “cocktail” that targets a suite of angiogenic factors. Izumi et al demonstrated that Herceptin, an antibody to Her2 has action on multiple antiangiogenic factors resulting in normalization. The expression of various angiogenic factors was examined in human breast tumors overexpressing Her2 using a gene array. It was observed that the expression of VEGF, transforming

endothelial growth factor ά, and plasminogen activator inhibitor -1 were increased and the expression of the anti-angiogenic factor thrombospondin-1 was increased when treated with Herceptin. It was also seen that with the treatment for Herceptin, the tumor tissue showed an increase in production of VEGF as compensation for the down regulation induced by Herceptin. This indicates a potential combination therapy of Herceptin and other antiangiogenic drugs (Izumi et. al., 2002).

Antiangiogenic therapy and oxygen perfusion

A hallmark of vascular normalization is the increase in tumor oxygenation resulting in radiosensitivity. Ansiaux et. al. (2006) reported a significant reoxygenation following treatment with SU5416, an antagonist to the VEGFR inhibiting binding of VEGF therefore reducing the formation of new vessels. This study showed an increase in tumor oxygen not as a result of remodeling of tumor vasculature, but rather as a result of a decrease in oxygen consumption by the tumor. An inhibition of mitochondrial respiration is responsible for the reoxygenation, independent of perfusion of the tumor, in which no significant change was observed between the treated and control groups. There was no observable histological change in the vasculature between the treated group and control group again indicating that a change in vessel architecture did not contribute to

the increased oxygen levels observed. It is important to note that the most significant increase in tumor oxygen was observed at day 2 after treatment and continued to decline thereafter. This again supports the idea that there is a window in which the application of radiation therapy will be most efficient. It was seen that after day 2, a significant tumor growth delay occurred when SU5146 was combined with radiation using 10 Gy. To rule out a direct sensitizing effect, tumors were irradiated in the presence of SU5146, and no significant delay in tumor growth was observed, indicating that the radiosensitivity was a result in the increase of oxygen during a particular time frame (Ansiaux et. al., 2006).

Combination therapy of ionizing radiation and thalidomide displayed a significant delay in tumor growth. Thalidomide has been showed by Asaiux et. al. (2005) to inhibit VEGF and bFGF and is widely tested in both preclinical and clinical studies. Statistically different tumor oxygen was seen in the control group and the group treated with thalidomide. At day 2 and 3 a maximum increase in tumor oxygen was observed. The tumors were irradiated on day 2 after the maximum oxygen levels were observed in order to study the oxygen effect. A significant increase in tumor growth delay was seen when tumors were irradiated two days following treatment with thalidomide. No tumor growth delay was observed *in vitro* when tumors were irradiated in the presence of thalidomide,

indicating the oxygen effect was the mechanism for the increased sensitivity to radiation (Ansiaux et. al., 2005).

As previously discussed work by Winkler et al using DC101, a monoclonal antibody against VEGFR2 Flk-1, showed a significant reduction in tumor hypoxia resulting in a window in which ionizing radiation is most efficient in delaying tumor growth. Treatment with DC101 alone in U87 human glioma xenographs produced no significant delay in tumor growth. Upon application of radiation beginning on day 4 to day 6 produced a remarkable increase in tumor growth delay. This is indicative again of the development of a window in which application of radiation will produce optimal results. The tumor growth delay coincided with the drop in tumor hypoxia seen in the tumors. Tumor hypoxia began to regress at day 2, and was nearly completely absent by day 5, and began to increase again by day 8 (Winkler et. al., 2004) .

Targeting Hypoxia with Bioreductive Drugs

In addition to exploiting the window of opportunity or increasing tumor oxygen tension to improve radiation therapy, it is also possible to exploit tumor hypoxia. Although tumor hypoxia presents several therapeutic barriers, the enzyme profile that is induced presents several drug targets, such as cytochrome c p450 reductase (cp450r) and

NAD(P)H oxidoreductase 1 (NQO1), detoxification enzymes involved in one and two electron reduction respectively (Patterson and Murray, 2002). Drugs that can be selectively activated through bioreduction by NQO1 and cp450r are known as bioreductive drugs (Seddon et. al., 2004). Quinones, specifically mitomycin C (MMC) served as the prototypical bioreductive drug (Beall and Winski, 2000; Stratford et. al., 2003). The premise behind bioreductive drugs is the introduction of a prodrug to be activated by cytochrome p450 reductase and is selective to a hypoxic environment. The inactive drug is activated by one electron reduction into a semiquinone radical that generates the cytotoxic species that reacts with DNA causing crosslinks (Boyle and Travers, 2006; Seddon et. al., 2004). The presence of oxygen causes auto-oxidation back to the parent compound rendering the drug inactive, making this class of drugs exclusively effective in hypoxic tumor environments. Other drugs in this class, E09 and RHI, are substrates of NQO1 and are activated by two-electron reduction. NQO1 is an oxygen independent reductase, which decreases the selectivity of drugs activated by this enzyme to a hypoxic environment. This mode of activation, however, is useful in hypoxic tissues because NQO1 is upregulated by hypoxia and allows for exploitation of

alterations in the genetic profile to improve therapeutic outcomes (Danson et. al., 2004; McKeown et. al., 2007; Patterson and Murray, 2002).

The Tumor Suppressor p53

The tumor suppressor gene p53 has been found to be mutated in more than half of all human cancers (Levine et. al., 1997). The p53 protein acts as a transcription factor that enhances the rate of transcription of several p53 target genes. The p53 protein is kept at low levels within the cell with a short half-life of about twenty minutes. When the cell encounters DNA damage, such as ionizing radiation, UV radiation, or chemical stress levels of p53 are increased within the cell and the half-life is lengthened by phosphorylation and binding to stabilizing proteins (Brown et. al., 2009). Once activated, p53 becomes activated as a transcription factor (Bitomsky et. al, 2009). The level of p53 is proportional the level of DNA damage in the cell. Levels of p53 can increase in response to various repair machinery, lead to cell cycle arrest or ultimately trigger cell death. P53 can also bind to excision repair damage sights and internal deletion loops (Norbury et. al., 2004).

The p53 protein contains 393 amino acids and has been structurally divided into 4 domains. The first 42 amino acids comprise the N-terminus and the transcriptionally

activation domain. The sequence DNA binding domain is composed of amino acids 102 to 292. This domain is protease resistant and contains a Zn^{2+} ion responsible for sequence specific DNA binding activity (Levine et. al., 1997; Norbury et. al., 2004). The DNA binding domain binds into a four and five stranded antiparallel β sheets that acts as a scaffold for two α- helices that bind directly to the DNA, forming a tetramer. More than 90% of the missense mutations occur in the DNA binding domain (Ward et. al., 2004). The C-terminal 24 amino acids comprise a protease sensitive domain that can bind both DNA and RNA depending on their sequences. The function of the C-terminal domain is to catalyze the re-association of single DNA and RNA breaks. p53 also bind to DNA ends as well as to internal deletion loops in DNA that have been generated by errors in replication and are subsequently detected and fixed by mismatch-repair machinery.

A major downstream event orchestrated by p53 is cell cycle regulation. In response to some forms of DNA damage, p53 activates the downstream target gene p21, which binds to a number of cyclin and Cdk complexes, blocking cell cycle progression into S phase. Activation of p21 in turn blocks cdk-4, blocking Rb, inhibiting E2F-1,2, thus preventing progression into S phase (Polager et.al., 2009). In response to extensive DNA damage, p53 transcriptionally activates BAX and BAK on the outer mitochondrial

membrane, leading to the formation of the mitochondrial outer permealization pore. Cytochrome c is released from the mitochondria and binds with the apoptosis protease activating factor 1 (APAF-1) forming the apoptosome, which in turn binds to the initiator caspase which is then cleaved, and then cleaves the effector caspase 3, leading to DNA fragmentation (Nayak et. al., 2009: Polager et. al., 2009).

Metabolic Reprogramming

Normal ATP generation occurs through the conversion of glucose molecules to pyruvate, and then further catabolism via the citric acid cycle and oxidative phosphorylation in the mitochondria. This means energy production yields 38 molecules of ATP per glucose molecule. Conversely, the generation of ATP from conversion of pyruvate to lactate yields only 2 ATP molecules per molecule of glucose. Tumors, regardless of their oxygen status, prefer the less effective mode of ATP production. Because of the marked inefficiency of glycolytic ATP production, glucose uptake has to increase in order to maintain energy levels to allow for proliferation and survival (Fukumura et. al., 2001; Fukumura and Jain, 2007)(Laconi, 2007; Shi et. al., 2001; Yu et. al., 2002). Increased glucose uptake is mediated by Hif-1, which increases expression of glucose transporters (GLUT1 and GLUT3) as well as key glycolytic enzymes. Hif-1 has

also been shown to repress oxidative phosphorylation by inhibiting the conversion of pyruvate to acetyl CoA for entry into the citric acid cycle. Hif-1 induces pyruvate dehydrogenase kinase 1 (PDK1), which inhibits pyruvate dehydrogenase (PDH), forcing pyruvate to be converted into lactate, ultimately suppressing pyruvate catabolism via the citric acid cycle, decreasing ATP formation through oxygen consuming oxidative phosphorylation (Gatenby et. al., 2006; Gillies and Gatenby, 2007; Gillies and Gatenby, 2007; Laconi, 2007; Shi et. al., 2001; Yu et. al., 2002). The gene encoding for lactate dehydrogenase A (LDH-A) is a HIF target gene. The protein lactate dehyrogenase A converts pyruvate to lactate and has been shown to be upregulated in colorectal cancers. LDH-A knockdowns have shown to have an increase in oxygen consumption and an increase in oxidative phosphorylation, decreasing the highly glycolytic tumor phenotype (Semenza, 2008; Shi et. al., 2001; Yu et. al., 2002). The production of lactate enables the tumor to regenerate NAD pools for ATP production, but the accumulation leads to a decrease in extracellular pH (pHe), leading to tumor acidosis. Lactate is extruded by the lactate/H^+ exchanger or monocarboxylate transporter (MCT4), which removes lactate from the cell, leading to a decrease in pH_e. This transporter is likely upregulated by a mechanism mediated by Hif-1. There is also a Na^+/H^+ exchanger (NHE1), also regulated

by Hif-1, which extrudes hydrogen ions from within the cell, keeping the intracellular pH (pH_i) at equilibrium. Accumulation of CO_2 as a byproduct from the conversion of pyruvate to lactate also contributes to the drop in extracellular pH. The membrane bound Hif-1 regulated enzyme carbonic anhydrase IX converts CO_2 to carbonic acid, which contributes to acidosis (Raghunand and Gillies, 2000; Williams et. al., 2004; Yu et. al., 2002).

Targeting Tumor Acidosis

Adaptation to the unstable tumor microenvironment involves the changes in the abundance or function of glycolytic enzymes to compensate for regions of hypoxia and defects in vascularization. These glycolytic changes result in intratumoral acidosis, which has shown to be advantageous for the survival of the tumor (Petrangolini et. al., 2006; Yu et. al., 2002). Microenvironmental pH has been linked to tumor invasion, metastasis and treatment resistance, supporting the notion that the mechanisms leading to resistance are of great clinical importance (Petrangolini et. al., 2006; Vaupel and Mayer, 2007; Yu et. al., 2002). One mechanism of increased aggressiveness and treatment resistance appears to be thorough HIF-1 mediated mechanisms. Shi et al showed that FG human pancreatic adenocarcinoma cells exposed to pH 6.7 had a marked increase in VEGF mRNA

expression measured by Northern blotting and indicates a role of tumor acidosis in angiogenesis (Shi et. al., 2001). These aggressive tumor cells also promoted degradation of the extracellular matrix (ECM) in MCF-10 human breast epithelial cells through an increase in the release of protolytic enzymes such as cathespin B, which promotes tumor invasion (Rozhin et. al., 1994). Tumor uptake of weak base drugs such as doxorubicin and vincristine are attenuated at low pH, introducing a therapeutic barrier and limiting treatment options. It has also been demonstrated by Anderson et al that an acidic pH_e leads to apoptotic and necrotic cell death of normal surrounding cells (Smallbone et. al., 2007), giving the tumor space in which to expand while the tumor cells acquire treatment resistance (Semenza, 2007).

Despite the resistance of acidic tumors to treatment**,** exploiting the tumor microenvironment has surfaced as a way to potentiate drug efficacy depending upon tumor phenotype. Enhancing pH_e has been used to increase the effect of weak acid drugs (Luciani et. al., 2004). Inducing hyperglycemia has proved an effective means of decreasing the difference in pH between tumors and normal tissue (Petrangolini et. al., 2006). Administration of glucose increases glycolytic flux, thereby increase the conversion of pyruvate to lactate, exacerbating tumor acidosis. Kuin et al demonstrated

that administration of a respiratory inhibitor m-iodobenzylguanidine (MIBG) decreases oxygen consumption and coupled with glucose treatment selectively acidified the extracellular tumor environment in RIF-1 tumor bearing mice (Kuin et. al., 1994). Burd et al demonstrated in mice bearing melanoma xenografts had an increase in oxygen tension of 2.8 mmHg to approximately 17 mmHg, and pH_e decreased from pH 6.7 to pH 6.3 (Burd et. al., 2001; Burd et. al., 2003) It has been demonstrated *in vitro* in several cell types that an increase in the (pH_i – pH_e) gradient increases uptake of weak acid drugs such as chlorambucil (Raghunand and Gillies, 2000).

Acidfication of pH_i is a technique used to enhance drug efficacy of weak acid drugs by enhancing pH_e and by disrupting the regulation of pH_i . Kuin et al treated CH3 mice bearing RIF-1 tumors with MIGB and glucose to decrease pH_e and then subsequently treated with amiloride to inhibit the Na^+/H^+ antiporter to prevent normalization of pH_i. A sensitization to melphalan and mitomycin C and decrease in tumor size was observed (Kuin et. al., 1994).

Selective alkalinization of extracellular tumor pH is a therapeutic approach to potentiate the use of weak base drugs. It has been demonstrated in CHO cells that a more basic extracellular pH is directly related to an increase in doxorubicin efficiency.

Raghunand et al measured intracellular and extracellular pH using ^{31}P MRS. It was demonstrated that chronic ad lib administration of water containing 200 mM $NaHCO_3$ to SCID mice inoculated with MCF-7 human xenografts showed an increase in both pH_e and pH_i . This alkalinization resulted in a 2-fold increase in tumor growth delay with doxorubicin compared to untreated controls, indicating a powerful role of alkalinization therapies (de et. al., 2009; Raghunand, 2006).

Prevention of extracellular acification through use of proton pump inhibitors (PPI) has proved an effective means to attenuate acidification and potentiate drug efficacy. An important mediator of pH homeostasis is the vacuolar H^+ ATPase ($V\text{-}H^+\text{-}ATPase$) that functions in pumping protons across the plasma membrane and a variety of intracellular organelles. The PPI esomeprazole decreased proliferation and caused rapid intracellular acidification, resulting in caspase-mediated cell death in melanoma cells. Dysregulation of intracellular pH homeostasis resulted in apoptosis *in vitro* and increased survival in mice bearing melanoma tumor xenografts (de et. al., 2009). Pretreatment with PPI omeprazole, esomeprazole, and pantoprazole sensitized melanoma and adenocarcinoma cells to cisplatin, 5-FU, and vinblastine. Pretreatment with PPI increased cytoplasmic drug retention and nuclear retention in the case of doxorubicin (Luciani et. al., 2004).

Inhibition of V-H^+-ATPase with Nik 12192, a PPI, increased the response of colorectal cells LoVo and HT29 to topotecan, increasing apoptosis and decreasing proliferation (Petrangolini et. al., 2006).

Summary

The physical properties of tumor neovasculature and the metabolic changes that occur in tumor cells present a significant challenge to tumor therapy. Therefore, it is hypothesized that the tumor microenvironment will induce signaling and enzymatic changes, which if manipulated or understood, could be used to improve treatment outcome. Furthermore, signaling and enzymatic profiles induced by the microenvironment can be exploited to improve response to therapies. The papers to be presented here focus on these proteins as central mediators of the adaptation and therapeutic response. To test these hypotheses, 3 major studies have been conducted. The first study entitled **"**Control of Glycolytic Flux by AMPK and p53-mediated Signaling Pathways in Tumor Cells Adapted to Low pH" tests the hypothesis that the acid microenvironment will induce signaling cascades and enzymatic changes to promote to survival. The second study "Maintenance of p53 homeostasis in tumor cells by riboflavin-stimulated NQO1 binding activity**"** tests the hypothesis that the nutrients and

co-factors in the tumor microenvironment can affect tumor survival and produce pro-tumorigenic conditions. The final study “Enhancement of the radiation response by exploiting the hypoxic tumor microenvironment” tests the hypothesis that the acidic and enzymatic properties can be manipulated to prevent or control tumors. It will be shown that central to the adaptation process there are three key proteins that are involved in signaling and enzymatic activity, p53, NQO1 and cp450r. These studies present a novel understanding of the microenvironmental adaptation process surrounding these proteins and provide mechanisms by which therapies could be developed to interfere with the adaptation process or exploit it. The results presented here could lead to the rational design of cancer therapies as well as preventative measures.

CHAPTER II: MATERIALS AND METHODS

Cell Culture

Early passage DB-1 melanoma cells and U87 glioblastoma cells were grown as monolayers at 37^0 C in humidified 5% CO_2 in α-MEM medium supplemented with 10% FBS, 12 mM glucose, 10 mL/L nonessential amino acids solution, and 2.9 g/L glutamine (α-MEM+). Low pH medium was prepared at pH 6.7 as described (Burd et. al., 2001). Cells were grown at pH 7.3 or grown at low pH conditions at pH 6.7. The 6.7 grown cells were adapted to growth at pH 6.7 for at least 14 days, but no more than 60 days before they were used in experiments. Acute acidification was for 48 hours. Riboflavin depletions experiments were conducted using custom riboflavin depleted α-MEM (Hyclone Thermo Scientific).

Animal and tumor models

U87 glioblastoma cells (American Type Culture Collection) were maintained in alpha MEM medium (Sigma) with 10% fetal bovine serum (Atlanta Biologicals). A U-87 cell suspension was injected subcutaneously into the right hind limb (5×10^5 cells in 100 μl PBS) of athymic NCR NUM mice (Taconic Farms).

Tumor growth delay

U-87 human glioblastoma cells were injected subcutaneously into the right hind limb of athymic NCR NUDE mice and allowed to grow to a hypoxic volume of ~550 mm^3 before treatment. EO9 or vehicle was administered 30 min. after each radiation

fraction on day 1, 2, and 3. The study used 4 treatment groups: vehicle (DMSO), radiation alone (Wachsberger et. al., 2004) (3 days x 7.5 Gy), EO9 (3 days x 2 mg/kg), and EO9 + radiation. EO9 was administered locally by intra-tumoral injection to achieve optimal delivery.

Transfections

Cells were transfected with a pcDNA3, 5.4 kb vector (Invitrogen, Carlsbad, CA) containing PFKFB3. PFKFB3 cDNA was amplified using a forward primer (5'-CGGGATCCATGCCGTTGGAACTGACG-3') and a reverse primer (5'-CCGCTCGAGTCAGTGTTTCCTGGAGGAG-3'). In the forward sequence the BamH I domain is underlined, and in the reverse sequence the XhoI domain is underlined. The FLAG™ sequence, Asp-Tyr-Lys-Asp-Asp-Asp-Asp-Lys, was used as the transfection marker.

Reagents

The AMPK inhibitor Compound C was obtained from EMD Chemicals and DMOG was obtained from Sigma. The riboflavin dicoumarol, cadmium sulfate, and protease inhibitor cocktail used in these studies were also obtained from Sigma.

Antibodies

Antibodies to phosphorylated AMPK, phosphorylated p53 (serines 15 and 392), NAMPT, PFKFB3, TIGAR, total mTOR and phosphorylated mTOR were used in the

dilution of 1:1,000. p53 and Bax was used in a dilution of 1:200. Anti-rabbit was used as a secondary at a dilution of 1:10,000 for phospho antibodies of phosphorylated AMPK, phosphorylated p53 (serines 15 and 392), Nicotinamide Phosphoribosyltransferase (NAMPT), PFKFB3, TIGAR, cytochrome p450 reductase, total mTOR and phosphorylated mTOR. Whereas an anti-mouse secondary was used for p53, actin, and GAPDH at a dilution 1:10,000. Anti-NQO1 primary antibody was used with a dilution of 1:10,000 and secondary anti-goat at a dilution of 1:10,000.

Glucose Consumption

A glucose detection kit (GHKB-2; Sigma), based on the enzymatic conversion of Glucose-6-Phosphate and NAD+ to 6-Phosphogluconate and NADH, measured the amount of glucose present in the samples. Cells were grown on T-25 culture flasks. When the cells were near confluency, the medium was removed and replaced with new 7.3 α-MEM+ without 12 mM glucose, or 6.7 α-MEM+. Enough 1 M-glucose solution was added to each flask to bring the final glucose concentration to 20 mM. Exactly 6 or 24 hours later, 50 μL aliquots of medium were removed from each flask. Subsequently each aliquot was then stored in an individual well of 96-well plate. The 96-well plate was then wrapped with Parafilm™ (Fisher) and placed in the freezer. In order to determine the rate of glucose consumption, the samples were successively diluted: 1) 10 μL of thawed sample:90 μL of deionized H2O, and 2) 10 μL from dilution 1:100 μL glucose assay reagent (G2020; Sigma). A 96-well plate spectrophotometer was then used

to determine the absorbance at 340 nm. An average absorbance was calculated based on the individual absorbance readings from each of the aliquots removed.

Glucose consumption after AMPK inhibition with Compound C was measured using an ACCU-CHECK^{TM} glucometer. U87 Cells were cultured in 6-well plates and treated with 10μM Compound C for 8 hours. Media samples were taking in 1 mL aliquots before and after Compound C treatment and were stored at -20°C until analyzed. Samples were thawed at 37 °C and read three times each.

Lactate Production

A lactate detection kit (826-UV; Sigma), based on the enzymatic conversion of lactate and NAD+ to pyruvate and NADH, measured the amount of lactate present in the samples. In order to determine the rate of lactate production, NAD (826-3; Sigma) was reconstituted as directed in the protocol (826-UV; Sigma). A [10:100] dilution of [sample (obtained from the glucose consumption assay 96-well plate):NAD solution] was prepared, and the absorbance at 340 nm was measured using a 96-well plate spectrophotometer. An average absorbance was calculated from the individual absorbance readings from each of the aliquots removed.

Western blotting

Cells grown in culture were washed twice with cold PBS and lysed with LDS sample buffer containing DTT added just prior to use. Buffer also contained aprotinin, AEBSF, sodium orthovanadate, and sodium fluoride to prevent degredation by proteases

and phosphatases. Western blotting was carried out with a total of 25 µg as quantified by Protein Dotmetrics kit (Applied Biosystems). Samples were run using 7% or 10% NUPAGE gels (Invitrogen Corp., CA, USA) using a Novex protein standard (Invitrogen). The proteins were transferred onto polyvinylidene difluoride membranes (Amersham Pharmacia Biotech, Piscataway, NJ). Western detection was carried out using CDP star from Tropix, Applied Biosystems (Chicago, IL, USA).

RNA isolation and real-time Reverse-Transcript Polymerase Chain Reaction (RT-PCR)

Homogenization of cells and isolation of RNA were performed using QIA shredder spin columns and an RNeasy Kit as instructed by the manufacturer (Qiagen, Valencia, CA, USA). 1 µg of RNA was reverse transcribed using a Super Script III Kit as instructed by the manufacturer (Invitrogen, Carlsbad, CA, USA) and diluted 1:5 for subsequent analyses. The following real-time reaction mix was prepared: 5 µl of diluted cDNA, 1 µl of mixed forward and reverse primers (10 µM each), 12.5 µl of SYBR Green (Qiagen), and nuclease-free water to a final volume of 25 µl. All real time RT-PCRs were run in triplicate for each cDNA sample using an iQ5 RT-PCR Detection System (BioRad, Hercules, CA, USA). Forty cycles of PCR were performed (95°C for 15seconds, 54°C for 30 seconds, 72°C for 30 seconds); fluorescence detection occurred during the 72°C step at each cycle. The data were analyzed using the $2^{-\Delta\Delta Ct}$ (Gallagher et. al., 2003) method and results were normalized to S15, which remains unchanged in response to treatment. Normalized values were plotted as relative fold over untreated. The following primers were purchased from Integrated DNA Technologies (Coralville, IA, USA): S15, Bax, and NQO1.

ROS Measurement

Cells in T-25 flasks were washed twice in PBS and pelleted by centrifugation. Cells were incubated with DCFA-DA at a final concentration of 100 μM in alpha MEM for 30 min at 37 °C. Cells were again pelleted and DCFA-DA medium was removed and fresh media added. Samples were analyzed by BD FACS flow cytometer.

Glutathione and Thioredoxin Reduction Assay

The cellular levels of glutathione (GSH) and thioredoxin were measured as described (Biaglow et. al., 2000). Briefly, cells in T-25 flasks after reaching ~85% confluency were gently washed twice PBS and suspended in PBS assay buffer containing Ca, Mg and K. Cells in buffer were treated with 16.7 mM glucose and 5mM final concentration of hydroxyethyl disulfide or Lipoate. A 100 μl of sample was taken every 15 min for 1 h and read on a spectrophotometer at 412 nm.

Annexin V-FITC staining

After treatment, adhered cell monolayers were trypsinized and washed twice with cold PBS. Apoptosis was determined using Annexin V-FITC apoptosis detection kit (R&D systems, MN, USA) as per manufacturer's instructions. 5×10^5 cells were resuspended in 100 μl of 1× binding buffer and mixed with 1 μl of Annexin V-FITC and 10 μl of propidium iodide. After 15 min incubation in the dark at room temperature, 400 μl of 1× binding buffer was added and the cells were analyzed using a BD FACS flow cytometer.

Oxygen Consumption

The rate of oxygen consumption was measured at 37^0 C, using a Clark electrode and amplifier (Yellow Springs Instrument Co., Yellow Springs, OH) as previously described in detail (23). A water bath was used to maintain a constant temperature, and cells were stirred continuously. MLA™ Brand pipettes (Fisher) were used to add cells and solutions to the chamber. MLA™ Brand pipettes were chosen because they cannot introduce air bubbles into the chamber by over-depressing the plunger.

Tumor Oxygen Measurements

Tumor oxygen tension was measured using the Oxford Oxylite fiberoptic probe (Oxford, England). The detection system is based on blue light excitation of ruthenium pigment at the end of a fiber optic probe, which is quenched by oxygen. Measurements were performed on anesthetized mice (75 mg/kg Ketamine and 0.3 mg/kg Acepromazine), while body temperature was maintained at 37°C with a heating pad. A 25-gauge needle was used to puncture the tumor capsule to facilitate insertion of the fiberoptic probe. The probe was guided into the tumor at a 2-4 mm depth.

Oxygen Consumption Measurements

Cells were rinsed with either pH 7.3 or pH 6.7 HEPES plus Ca, Mg and K (HEPES+) to remove any remaining medium. The cells were then harvested, by scraping, using 6 mL of HEPES(+) per flask. All harvested cell suspensions were

combined into one centrifuge tube, and centrifuged for 6 min at 1500 rpm at 6^0 C. After centrifugation, the buffer was aspirated from the pellet, and the pellet was re-suspended in 120 μL of fresh HEPES(+).

For each experimental trial, 30 μL of cell suspension were placed in the oxygen consumption chamber and a basal rate of oxygen consumption was measured prior and after addition of 5 μL of either HEPES(+), 16.7 mM glucose, 100 μM dinitrophenol (DNP). (The basal rate is defined as the rate of oxygen consumption of cells in buffer, prior to an addition of another solution.) The rate of oxygen consumption was then measured after addition of an agent.

A 100 μL aliquot of the cell solution was removed from the chamber after the second 5-min interval, and stored in an Eppendorf tube (Fisher) in the freezer until a protein determination could be conducted.

Immunoprecipitations

Following treatment, cells grown in culture were washed twice with ice cold PBS and then were lysed with ice cold NP-40 buffer substituted with 1% Triton X, 150 mM NaCl, and 50 mM tris HCL. Protease inhibitor cocktail, NaF, and NaV were added immediately before use. Lysates were immunoprecipitated with 4μl anti-NQO1 antibody overnight at 4°C with gentle agitation. Lysates were then incubated with 50 μl Protein G bead slurry (Sigma) for 1 hr at 4°C on a rocking platform. Beads were then pelleted by centrifugation and washed three times with buffer. LDS sample buffer was then added to beads and samples boiled for 10 min at 100 °C, and supernatant was removed.

NQO1 Enzymatic Assay

Protocol for measurement of NQO1 activity was adapted from Ernster et al (Ernster et. al., 1962). Cells were grown in culture and NQO1 activity was inhibited with 400 μM dicoumarol for 4 hr. Adhered monolayers were washed twice with cold PBS and then lysed with .05% Triton-X containing protease inhibitor cocktail added immediately before used. Cells were put through 3 rapid freeze thaw cycles and the insoluble fraction was removed by centrifugation. Lysates were treated with 20 μM riboflavin for 1 hr at 4°C on a rotating platform. Standard reaction mixture contained 77 μM cytochrome c (Sigma), 200 μM NADH (Sigma), 10 μM menadione (Sigma), 0.14% BSA (Sigma); all dissolved in 50 mM tris HCL adjusted to pH 7.5. Assay was measured using a kinetic protocol on an ULTRAMARK BioRad Imaging Microplate System at 550 nm at 25 °C.

Cellular Proliferation Assay

Cells grown in 6-well culture plates were trypsinized and pelleted via centrifugation, then counted using a hemocytometer following trypan blue staining. Only viable cells were counted and used in cell number analysis.

Tumor growth statistics

Mixed–effects regression was used to model the base-10 logarithm of tumor volume as a function of time and treatment (tumor growth analyses). The

log-transformed outcome was used because tumors of this size grow approximately exponentially, and therefore the logarithm of the tumor volume is approximately linear over time. This approach appropriately handles unbalanced data, such as a different number of measurements for different animals, and takes into account the correlation of each animal's measurements over time. These analyses were carried out with SAS 8.2 (SAS Institute Inc., Cary, NC, 1999-2001).

Statistical Analysis

All measurements represent the mean of three different experiments with three values of each + SE or SD where indicated. Statistical significance was evaluated using a student's t-test and values noted as significant with * when $p < .05$, ** when $p < 0.01$-0.001, and *** when $p < 0.001$.

CHAPTER III: CONTROL OF GLYCOLYTIC FLUX BY AMPK AND P53 MEDIATED SIGNALING PATHWAYS IN TUMOR CELLS ADAPTED TO LOW PH

Abstract

Tumors cells grow in nutrient and oxygen deprived microenvironments and adapt to the suboptimal growth conditions by altering their metabolic pathways. This adaptation process commonly creates a tumor phenotype which displays a high rate of anaerobic glycolysis and aggressive tumor characteristics. The glucose regulatory molecule, 6-Phosphofructo-2-Kinase/Fructose-2,6-Biphosphatase 3 (PFKFB3), is a bifunctional enzyme that is central to glycolytic flux and is downstream of the metabolic stress sensor AMP-activated protein kinase (AMPK), which has been shown to activate an isoform of PFK (PFK-2). As hypothesized, our results demonstrated that chronic low pH exposure induced AMPK activation which resulted in the upregulation of PFKFB3 and p53, and the downregulation of mammalian Target Of Rapamycin (mTOR) in two tumor cell lines, DB-1 Melanoma and U87 Glioma. Conversely, inhibition of AMPK resulted in downregulation of PFKFB3 and inhibited glycolysis. When PFKFB3 was over-expressed in DB-1 tumor cells, it induced a high rate of glycolysis and inhibited oxygen consumption. In contrast, low pH-adaptated cells did not display increased glycolysis after PFKFB3 induction because TP53-induced Glycolysis and Apoptosis Regulator (TIGAR) was increased with low pH. Low pH –adapted cells were also resistant to apoptosis, despite upregulation of p53. This may be partially explained by the induction of anti-apoptotic proteins and TIGAR's ability to reduce lactate production.

These fundamental results indicate that low pH activates AMPK and induces a high glycolytic and apoptotic potential that is countered by TIGAR and anti-apoptotic proteins, respectively. The control of glycolysis thus minimizes acidification and further protects tumor cells from death.

Introduction

Tumors experience dynamic microenvironmental changes that require them to adapt or parish. Tumors often adapt by altering their own metabolism in order to survive, although the mechanisms of these metabolic modifications are not well characterized. A well known phenotype resulting from this adaptive ability has been repeatedly demonstrated by the positive correlation between anaerobic glycolysis (both independent and dependant of cellular oxygen tension) and the level of aggressiveness in tumors (Gatenby and Gillies, 2004). It is generally accepted that tumor cells are able to offset the decreased energy production that occurs when switching from aerobic to anaerobic glycolysis by increasing overall glucose usage (Di et. al., 1987; Mathupala et. al., 2007; Minchenko et. al., 2002). Additionally, anaerobic glycolysis results in the production of lactic acid which cannot undergo mitochondrial oxidation and must, therefore, be extruded from the cell (Smallbone et. al., 2007). Lactic acid accumulation also leads to decreased localized (intracellular and/or extracelluar) pH and, subsequently, increased malignancy and chemotherapeutic resistance (Smallbone et. al., 2005). Therefore, it is reasonable to propose that tumor cells may regulate this malignant survival pathway by modulating the expression and activity of key glycolytic enzymes.

The glucose regulatory molecule, 6-Phosphofructo-2-Kinase/Fructose-2,6-Biphosphatase 3 (PFKFB3), is a bifunctional enzyme, where the Phosphofructo-2-Kinase (PFK) domain functions to promote glycolysis and the fructose-2,6-biphosphatase domain functions to catalyze the reverse reaction (Pozuelo et. al., 2003). AMP-Activated Protein Kinase (AMPK) has been shown to activate an isoform of PFK-2, PFKFB2 via

phosphorylation of serine 466 in heart tissue (Marsin et. al., 2000). This enzymatic stimulation of glycolysis leads to both increased glycolytic ATP and lactate production. We propose that this same pathway is at work in tumor cells, which would promote glycolysis and resistant phenotypes.

AMPK functions as a cellular energy meter and its activity increases as the ratio of AMP:ATP decreases and when aerobic conditions arise. When a cell is under metabolic stress AMPK works to halt the anabolic processes that require ATP, such as protein synthesis and cell proliferation, and to increase pathways that produce ATP, such as glycolysis (Marsin et. al., 2000; Thoreen and Sabatini, 2005). Alternately AMPK can lead to activation of the tumor suppressor p53. Activation of p53 has been coupled with AMPK's subsequent ability to inactivate the mammalian Target Of Rapamycin (mTOR) cell proliferation pathway, which is a likely mechanism by which AMPK exerts its proapoptotic effects (Drakos et. al., 2009; Thoreen and Sabatini, 2005; Weyergang et. al., 2009). AMPK acts as a stress sensor so microenvironmental dysregulation of metabolism by acute or chronic changes in pH is likely to affect its activation and that of subsequent downstream pathways.

Tumor cells that adapt to acute and chronic low pH conditions must increase hydrogen ion extrusion or reduce lactate production in order to prevent fatally low pH levels. For example, when pH becomes acutely or low, tumor cells can quickly decrease the rate of glycolysis and lactate production (Burd et. al., 2001). Although a decrease in glycolysis can spare acidosis, cellular bioreduction pathways are closely linked to glucose flux, so changes in glycolysis can alter the bioreduction capacity of tumor cells by

bypassing the Pentose-Phosphate Pathway (PPP). When bioreduction pathways are decreased and Reactive Oxygen Species (ROS) are elevated the TP53-induced Glycolysis and Apoptosis Regulator (TIGAR) molecule is upregulated. TIGAR shares fructose-2,6-biphosphatase's PFK antagonistic functions and is able to promote the glycolysis-opposing reaction that converts fructose-1,6-phosphate to fructose-6-phosphate. This reverse reaction leads to accumulation of fructose-6-phosphate and glucose-6-phosphate, which are then shunted into the PPP in order to restore bioreduction capacity (Bensaad et. al., 2006; Bensaad et. al., 2009).

Here we report a novel metabolic adaptation response induced by low pH adaptation and describe mechanisms *in vitro* that would predict tumorigenesis and treatment resistance as seen in clinical settings. We describe the relationship between low pH and glycolytic flux, which involves AMPK and p53-mediated pathways, including the upregulation of PFKFB3. We also purpose that the upregulation of TIGAR may be one mechanism by which tumor cells are able to prevent lethal H^+ accumulation in chronic low pH environments.

Materials and Methods

Cell Culture

Early passage DB-1 melanoma cells were grown as monolayers at 37^0 C in humidified 5% CO_2 in α-MEM medium supplemented with 10% FBS, 12 mM glucose, 10 mL/L nonessential amino acids solution, and 2.9 g/L glutamine (α-MEM+). Low pH medium was prepared at pH 6.7 as described (Burd et. al., 2001). Cells were grown at pH 7.3 or grown at low pH conditions at pH 6.7. The 6.7 grown cells were adapted to growth at pH 6.7 for at least 14 days, but no more than 60 days before they were used in experiments. Acute acidification was for 48 hours.

Transfections

Cells were transfected with a pcDNA3, 5.4 kb vector (Invitrogen, Carlsbad, CA) containing PFKFB3. PFKFB3 cDNA was amplified using a forward primer (5'-CGGGATCCATGCCGTTGGAACTGACG-3') and a reverse primer (5'-CCGCTCGAGTCAGTGTTTCCTGGAGGAG-3'). In the forward sequence the BamH I domain is underlined, and in the reverse sequence the XhoI domain is underlined. The FLAG™ sequence, Asp-Tyr-Lys-Asp-Asp-Asp-Asp-Lys, was used as the transfection marker.

Rate of Glucose Consumption

A glucose detection kit (GHKB-2; Sigma), based on the enzymatic conversion of Glucose-6-Phosphate and NAD+ to 6-Phosphogluconate and NADH, measured the

amount of glucose present in the samples. Cells were grown on T-25 culture flasks. When the cells were near confluency, the medium was removed and replaced with new 7.3 α-MEM+ without 12 mM glucose, or 6.7 α-MEM+. Enough 1 M-glucose solution was added to each flask to bring the final glucose concentration to 20 mM. Exactly 6 or 24 hours later, 50 μL aliquots of medium were removed from each flask. Subsequently each aliquot was then stored in an individual well of 96-well plate. The 96-well plate was then wrapped with Parafilm™ (Fisher) and placed in the freezer. In order to determine the rate of glucose consumption, the samples were successively diluted: 1) 10 μL of thawed sample:90 μL of deionized H2O, and 2) 10 μL from dilution 1:100 μL glucose assay reagent (G2020; Sigma). A 96-well plate spectrophotometer was then used to determine the absorbance at 340 nm. An average absorbance was calculated based on the individual absorbance readings from each of the aliquots removed.

Total glucose consumption after AMPK inhibition with Compound C was measured using an ACCU-CHECK^{TM} glucometer. U87 Cells were cultured in 6-well plates and treated with 10μM Compound C for 8 hours. Medium samples were taken in 1 mL aliquots before and after Compound C treatment and were stored at -20°C until analyzed. Samples were thawed at 37 °C and read three times each.

Lactate Production

A lactate detection kit (826-UV; Sigma)*, based on the enzymatic conversion of lactate and NAD+ to pyruvate and NADH, measured the amount of lactate present in the samples. In order to determine the rate of lactate production, NAD (826-3; Sigma) was

reconstituted as directed in the protocol (826-UV; Sigma). A [10:100] dilution of [sample (obtained from the glucose consumption assay 96-well plate):NAD solution] was prepared, and the absorbance at 340 nm was measured using a 96-well plate spectrophotometer. An average absorbance was calculated from the individual absorbance readings from each of the aliquots removed.

Western Blotting

Western blotting was carried out with a total of 25 μg of each sample in 7% and NUPAGE gels (Invitrogen Corp., CA, USA). Antibodies to phosphorylated AMPK, phosphorylated p53 (serines 15 and 392), NAMPT, PFKFB3, TIGAR, total mTOR and phosphorylated mTOR were used in the dilution of 1:1000. p53 and Bax was used in a dilution of 1:200. Anti-rabbit was used as a secondary at a dilution of 1:10000 for phospho antibodies of phosphorylated AMPK, phosphorylated p53 (serines 15 and 392), Nicotinamide Phosphoribosyltransferase (NAMPT), PFKFB3, TIGAR, total mTOR and phosphorylated mTOR. Whereas anti-mouse was used for p53 and actin at a dilution 1:10000. Western detection was carried out using CDP star from Tropix, Applied Biosystems (Chicago, IL, USA).

ROS Measurement

Cells in T-25 flasks were washed twice in PBS and pelleted by centrifugation. Cells were incubated with DCFA-DA at a final concentration of 100 μM in alpha MEM

for 30 min at 37 °C. Cells were again pelleted and DCFA-DA medium was removed and fresh medium added. Samples were analyzed by BD FACS flow cytometer.

Glutathione and Thioredoxin Reduction Assay

The cellular levels of glutathione (GSH) and thioredoxin were measured as described (Biaglow et. al., 2000). Briefly, cells in T-25 flasks after reaching ~85% confluency were gently washed twice with PBS and suspended in PBS assay buffer containing Ca, Mg and K. Cells in buffer were treated with 16.7 mM glucose and 5mM final concentration of hydroxyethyl disulfide or Lipoate. A 100 µl of sample was taken every 15 min for 1 h and read on a spectrophotometer at 412 nm.

Annexin V-FITC staining

U87 cells were irradiated with 5 and 10 Gy following chronic acidification. After treatment, these cells were allowed to proliferate for 24 hours before measuring apoptosis. Apoptosis was determined using an Annexin V-FITC apoptosis detection kit (R&D systems, MN, USA) as per manufacturer's instructions. 5×10^5 cells were resuspended in 100 µl of 1× binding buffer and mixed with 1 µl of Annexin V-FITC and 10 µl of propidium iodide. After 15 min incubation in the dark at room temperature, 400 µl of 1× binding buffer was added and the cells were analyzed using a BD FACS flow cytometer.

Oxygen Consumption

The rate of oxygen consumption was measured at 37^0 C, using a Clark electrode and amplifier (Yellow Springs Instrument Co., Yellow Springs, OH) as previously described in detail (23). A water bath was used to maintain a constant temperature, and cells were stirred continuously. MLA™ Brand pipettes (Fisher) were used to add cells and solutions to the chamber. MLA™ Brand pipettes were chosen because they cannot introduce air bubbles into the chamber by over-depressing the plunger.

Cells were rinsed with either pH 7.3 or pH 6.7 HEPES plus Ca, Mg and K (HEPES+) to remove any remaining medium. The cells were then harvested, by scraping, using 6 mL of HEPES(+) per flask. All harvested cell suspensions were combined into one centrifuge tube, and centrifuged for 6 min at 1500 rpm at 6^0 C. After centrifugation, the buffer was aspirated from the pellet, and the pellet was re-suspended in 120 μL of fresh HEPES(+).

For each experimental trial, 30 μL of cell suspension were placed in the oxygen consumption chamber and a basal rate of oxygen consumption was measured prior and after addition of 5 μL of either HEPES(+), 16.7 mM glucose, 100 μM dinitrophenol (DNP). (The basal rate is defined as the rate of oxygen consumption of cells in buffer, prior to an addition of another solution.) The rate of oxygen consumption was then measured after addition of an agent.

A 100 μL aliquot of the cell solution was removed from the chamber after the second 5-min interval, and stored in an Eppendorf tube (Fisher) in the freezer until a protein determination could be conducted.

Statistical Analysis

All measurements represent the mean of three different experiments with three values of each $\pm$ SE or SD where indicated. Statistical significance was evaluated using a student's t-test and values noted as significant with * when $p < .05$, ** when $p < 0.01$-0.001, and *** when $p < 0.001$.

Results

Low pH Induces PFKFB3 and Phosphorylated AMPK

We have previously shown that cells exposed to acute or chronic low pH had decreased rates of glycolysis and increased rates of oxidative phosphorylation compared to cells grown at pH 7.3. However, no mechanism has been proposed for this change in energy metabolism. Therefore, we investigated the effect of acute and chronic low pH on the glycolytic enzyme PFKFB3 which has been shown to be a key regulatory enzyme in tumor cells (Chesney et. al., 1999). PFK2FB3 was elevated by both acute and chronic low pH (Figure 3.1 A). This upregulation was also confirmed in U87 glioma cells (Figure 3.1 C). AMPK is a stress sensor and it has been shown that it can increase the activity of PFKFB2 in heart tissue (Marsin et. al., 2000). We therefore hypothesized that the stress of acute or chronic exposure to low pH would induce the activation of AMPK. As anticipated, we did observe that phosphorylated AMPK was elevated in both acutely and chronically acidified DB-1 and U87 cells (Figure 3.1 B, D, E).

To confirm the role of PFKFB3 in glycolysis, PFKFB3 was over-expressed in DB-1 melanoma cells (Fig 3.2 A). In contrast to previous findings with acute and low pH adapted cells (Burd et. al., 2001), over-expression of PFK-2 increased the rate of glycolysis and lactate production (Figure 3.2 B-C). Furthermore, compared to vector control cells, the rate of oxygen consumption was decreased in DNP treated cells (Figure 3.2 D-E). The decreased rate of oxygen consumption indicates a role for PFKFB3 in maintaining high glycolytic flux by shunting glucose into the glycolytic pathways and thus decreasing rates of oxidative phosphorylation. Taken together, these results suggest

that PFKFB3 is a key modulator of the high rate of glycolysis and reduced rates of oxidative phosphorylation observed in many tumors. Further, the low pH adaptation process induced mechanisms to counter the additional PFKFB3, likely in an attempt to resist acidosis through metabolic stasis. We therefore investigated potential mechanisms for this observation.

Induction of ROS

Both glycolysis and pH are critically linked to cellular redox status. More recently the role of ROS modulating signaling pathways has proven important (Drakos et. al., 2009; Thoreen and Sabatini, 2005). For that reason we investigated the effect of low pH on GSH and thioredoxin bioreduction pathways. We observed that DB-1 cells grown at pH 6.7 had decreased bioreductive capacity as measured by GSH bioreduction compared to cells grown at pH 7.3 (Figure 3.3 A). The GSH bioreduction capacity in low pH-adapted cells was not affected by acute acidification until exposed to extremely low pH at 6.0. Cells grown at pH 7.3 exhibited greater GSH bioreduction, but had a sensitivity to acute pH change. Thioredoxin also appeared to be unaffected by acute low pH exposure in 7.3 grown cells (Figure 3.3 B). As bioreduction capacity was reduced, an increase in total ROS as measured via DCFA-DA staining was observed in acutely and chronically acidified DB-1 cells (Figure 3.3 C) as compared to normal pH cells. Total ROS production was also increased in acutely and chronically acidified U87 cells as well (Figure 3.3 D). This result supports the notion that there is a global decrease in bioreductive capacity in response to acute and chronic acidification.

AMPK Activation and ROS Can Inhibit MTOR

The mTOR pathway is a downstream stress response pathway that conserves energy by reducing cell proliferation and protein synthesis. Both AMPK activation and ROS can lead to the inhibition of mTOR (Drakos et. al., 2009; Thoreen and Sabatini, 2005). In both acutely (Figure 3.4 A) and chronically (Figure 3.4 B) acidified cells mTOR was downregulated. In concert, there was a 1.5 fold decrease in total cell number after 48 hours at pH 6.7 compared to pH 7.3 control cells (Figure 3.4 C). This coincides with the downregulation of mTOR and indicates multiple pathways are involved in the adaptation process and that the metabolic effects of low pH adaptation can lead to a static metabolism cell phenotype.

Low pH Induces p53 Activation and the Downstream Target TIGAR

In addition to pH, other molecular antagonists of glycolysis were investigated. Because ROS were induced and mTOR was inhibited, we investigated the activation of p53 through phosphorylation of its tetramerization site at serine 392. In chronically adapted low pH cells ser 392 phosphorylation was elevated (Figure 3.5 A). Tetramerization of p53 at ser 392 induces its transcriptional activity so we looked at downstream targets. The anti-glycolytic antagonist TIGAR, which is a target of p53, was also elevated in chronically acidified DB-1 cells (Figure 3.5 A). Upregulation of both TIGAR and p53 was confirmed in U87 cells (Figure 3.5 B-C). Despite the presence of p53, Bcl-2 and another AMPK dependent protein, Nampt, was also elevated in

chronically adapted low pH cells (Figure 3.5 D). Presence of another p53 antagonist ΔNp73 was also upregulated in chronically acidified cells (Figure 3.5 F). Nampt has been shown to contribute to mitochondrial preservation under stress conditions, including oxidative stress. To confirm the anti-apopototic profile conferred therapeutic resistance we investigated the effect of adaptation on the radiation response. The 7.3 grown cells were sensitive to radiation-induced apoptosis. However, the low pH adapted cells were significantly more resistant to radiation than their 7.3 grown counterparts (Figure 3.5 E).

To confirm that AMPK upregulated PFKFB3 and activates p53 the low pH adapted cells were treated with Compound C, which inhibits AMPK. After treatment with Compound C for 8 hrs., PFKFB3 and phosphorylated p53 were downregulted (Figure 3.6 A). Compound C treatment alone resulted in significantly lower rates of glycolysis (Figure 3.6 B). There was no increase in apoptosis or radiation sensitivity of Compound C-treated cells (data not shown); however a significant increase in non-apoptotic cell death was observed 72 hrs later (Figure 3.6 C). Treatment with Compound C also decreased induction of ΔNp73 in chronically acidified cells (Figure 3.6 D). It is probable that cell death was p53 independent as apoptosis was not increased and activated p53 was reduced.

Discussion

Low pH Induced AMPK and PFKFB3

Our results demonstrate for the first time that low pH-adaptation induces PFKFB3, which likely results from AMPK activation. AMPK is induced when the ratio of AMP/ATP increases as a result of decreased ATP production. This cellular energy deficiency is often a result of changes in glycolysis and oxidative phosphorylation (Kuhajda, 2008). In spite of PFKFB3 upregulation, we did not see increased glycolysis in low pH adapted cells. This finding is consistent with previous work from our group which demonstrated that adaptation to low pH significantly reduces glycolysis and increases oxidative phosphorylation (Burd et. al., 2001). Others have also shown that a reduction in pH can reduce the energy status of cells (Song et. al., 1980). This indicates that low pH induces a metabolic stasis on tumor cells which may be able to facilitate resistance to acidification and increased radioresistence (Burd et. al., 2001; Burd et. al., 2003). This stasis appears to be mediated through the antagonism or inactivation of PFKFB3, as overexpression induces the opposite effects.

The low-pH induction of PFKFB3 is also consistent with previous studies (Atsumi et. al., 2002) showing an upregulation of PFKFB3 in tumors in vivo. To this end we have previously shown that low pH adapted tumor cells in vivo resist acidification by reducing glycolytic rates (Burd et. al., 2001; Burd et. al., 2003). Our results here indicate that two mechanisms are likely responsible for the decrease in glycolysis. First low pH can reduce enzyme activities and external H^+ gradients can reduce extrusion (Song et. al., 1980). Tumor cells commonly upregulate the H^+ extrusion mechanism, which involves a

Na^+/H^+ anti-porter. This anti-porter expels hydrogen ions and can then achieve near-normal internal pH (pHi), while still coping with a low external pH. However, acute changes can overwhelm this system and drop the pHi and correspondingly reduce enzyme activities. It was also observed that TIGAR was upregulated (Figure 3.5 A-B) following long-term and chronic pH adaptation. Therefore it is likely that acute changes in pH would produce immediate and transient changes in glycolysis, but chronic changes would involve additional changes such as the upregulation of TIGAR, which has been shown to reduce the rate of glycolysis and ROS in tumor cells (Schematic 3.1).

Inhibition of Glycolysis and Bioreduction Capacity

The upregulation of TIGAR is usually associated with the reduction of ROS as glucose is shunted into the PPP by inhibition of PFK1 (Schematic 3.1). However, we observed a marked increase in ROS by acute and chronic acidicifcation. This was consistent with the observation that bioreduction capacity was reduced in low pH adapted cells compared to 7.3 grown cells. Furthermore, decreasing pH acutely in 7.3 grown cells reduced GSH levels (Figure 3.3 A) indicating that glutathione bioreduction was pH sensitive in these cells. In contrast, bioreduction in the 6.7 adapted cells appeared independent of pH, and raising the pH in the 6.7 grown cells to 7.3 did not restore bioreduction. If one assumes that the PPP is functional and TIGAR is actively shunting glycolytic metabolites into the PPP, it is conceivable that the PPP simply shifts from the oxidative phase to the non-oxidative phase. This would increase DNA synthesis and would be consistent with an observation that low pH adapted cells have higher DNA repair rates compared to cells grown at normal pH (Song et. al., 1980). Furthermore, this

observation is consistent with previous studies that show tumor cells are susceptible to glucose deprivation because they utilize glycolysis to decrease ROS (ykin-Burns et. al., 2009).

AMPK Activation and ROS Can Inhibit MTOR and Induce p53

The induction of AMPK in the low pH response may play important roles in the resistance to apoptosis. For example the induction of AMPK leads to mTOR inhibition via inhibition of the Tuberous Sclerosis Complex Protein 1/2 complex. Inhibition of mTOR can lead to activation of autophagy to allow cells to survive long periods of time during high levels of stress (Rouschop and Wouters, 2009). DB-1 cells were resistant to apoptosis following radiation treatment. This has also been observed in the clinical setting (Davids et. al., 2009) and it had been proposed that such resistance may be a result of autophagy. The autophagic process involves the self consumption of long-lived proteins and cytoplasmic organelles, which are then used for synthesis of ATP and macromolcules to compensate for a low energy, low nutrient environment (Bohensky et. al., 2009; Zhuang et. al., 2009). Activation of AMPK and subsequent repression of mTOR seen in the chronically adapted low pH system may induce an autophagic protective response, leading to metabolic stasis and resistance to ionizing radiation as we observed (Figure 3.5 E).

It has been previously shown that both AMPK activation and the inhibition of mTOR can induce p53 (Marsin et. al., 2000). In addition, ROS increases DNA damage and can also cause the activation and induction of p53. These results indicate that p53 is

activated in the low pH adapted cells and AMPK and ROS likely play a role in its stabilization. Acidification can select for cells that express mutated p53 (Williams et. al., 1999), however, the studies here present p53 as a functional and important transcription factor. The stabilization of p53 appears to be important in the adaptation process as it induces its downstream target TIGAR. The expression of p53 is usually associated with anti-tumor activity, and many melanoma tumors have functional, unmutated p53 but bypass its pro-apoptotic effects by expressing antagonists, such as deltaN p73 (Melino et. al., 2002). It has even been demonstrated that p53 induces deltaN p73 which can counter the effects of another anti-tumor molecule, p73 (Thangasamy et. al., 2007). We have shown that in DB-1 cells p73 is upregulted by p53 (manuscript in revision). BCL-2 alone cannot rescue cells from acidification (Hague et. al., 1998), however, the anti-apoptotic protein BCL-2 was upregulated in these cells and likely works in conjunction with other anti-apoptotic responses as well as reduced acidification (Burd et. al., 2003).

In glioma, however, p53 is also predominantly wildtype and a high level of DNA repair is the primary treatment barrier (Bao et. al., 2006). We observed a slight elevation of the AMPK dependent protein Nampt in low pH adapted U87 cells (Figure 3.5 D). Nampt is a survival protein that is responsible for maintaining both the NAD bioreductive pool, and mitochondrial NAD levels. Importantly, Nampt specifically provides NAD for the DNA repair enzyme Parp-1, which has been found to be a primary treatment barrier in glioma (Bao et. al., 2006) and may be involved in the radioresistence observed in our low pH system. These results are also consistent with many reports that indicate low pH adapted cells are resistant to apoptosis or therapy (Park et. al., 2000). The glioma cells

tested here were highly resistant to radiation induced apoptosis. Therefore, the upregulation of p53 is offset by the upregulation of various anti-apoptotic genes or additional p53 antagonists, which shift gene expression from apoptotic to pro-tumorigenic expression profiles.

Conclusion

The novel data presented here demonstrates that exposure to chronic low pH conditions activate AMPK which in turn mediates several metabolic events. It was also demonstrated that PFKFB3 is a potent glycolytic enzyme and its expression was upregulated in response to pH adaptation. However PFKFB3 expression in low pH adapted cells did not result in a high rate of glycolysis. This lack of glycolytic response is likely due to low pH decreasing global enzymatic activity along with the induction of TIGAR. Further, these results indicates that the tumor suppressor p53 could play a central role in adaptation. Taken together, these results indicate that targeting AMPK or other downstream protein could have profound role in improving therapy, as well as give insight into malignant transformation related to decreased microenvironmental pH.

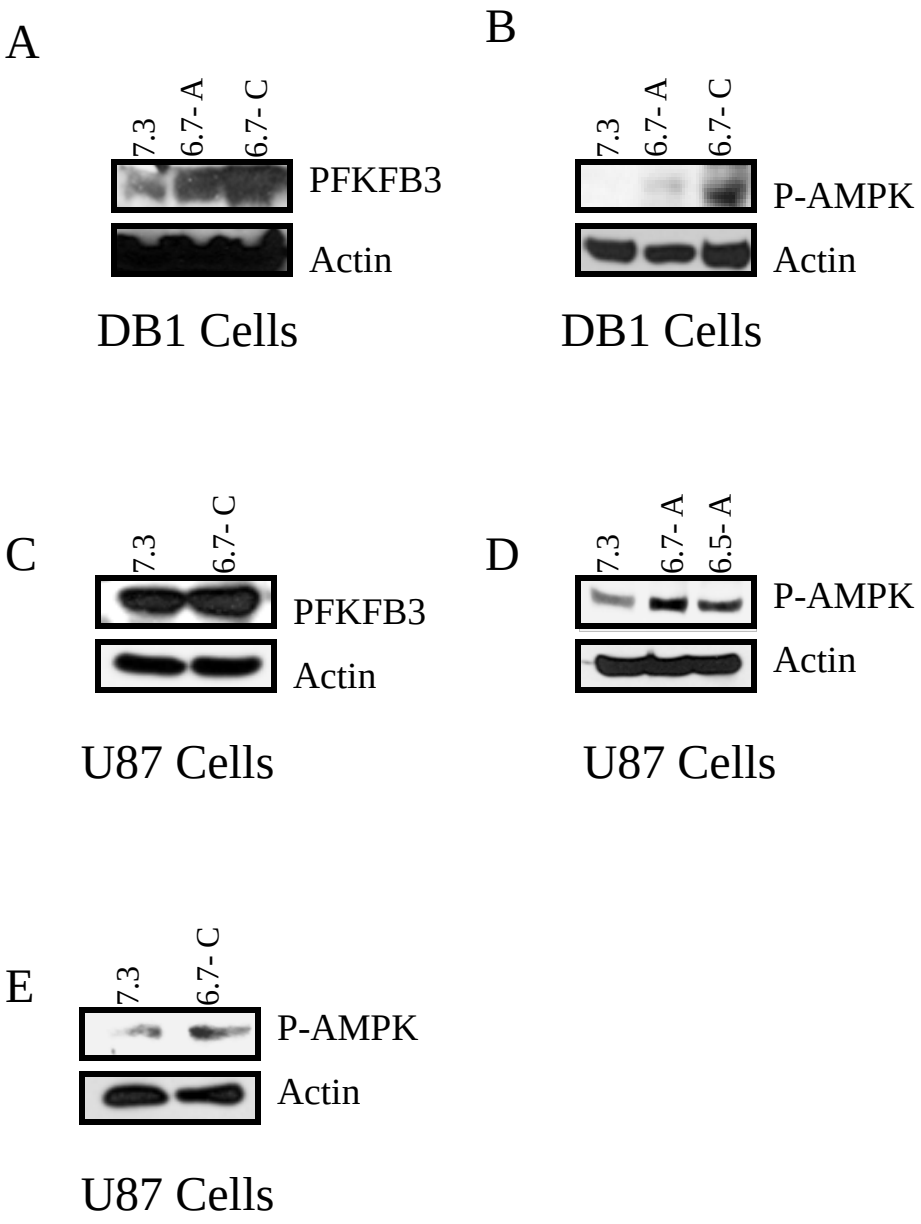

Figure 3.1. Expression of phosphorylated AMPK and PFKFB3 in acutely and chronically acidified DB-1 and U87 cells. Western blot of (A) PFKFB3 and (B) phosphorylated AMPK in acutely and chronically acidified DB-1 cells. Western blot of PFKFB3 (C) and phosphorylated AMPK (D-E) in chronically acidified U87 cells. Blots are representative of at least 3 independent experiments.

A

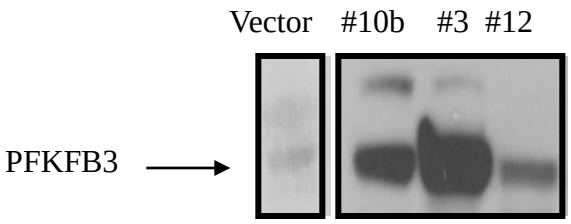
Vector
#10b
#3
#12
PFKFB3

B

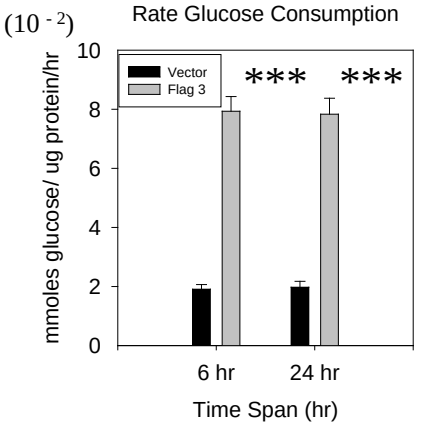
Rate Glucose Consumption
(10 - 2)
mmoles glucose/ ug protein/hr
Vector
Flag 3
***
***
0
2
4
6
8
10
6 hr
24 hr
Time Span (hr)

C

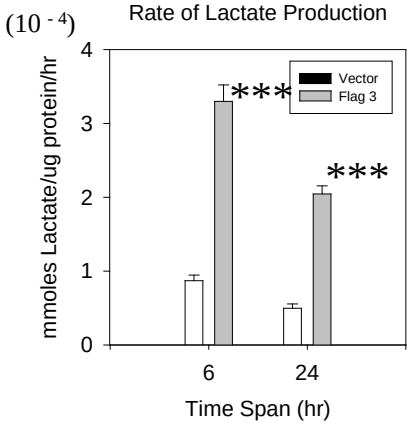
Rate of Lactate Production
(10 - 4)
mmoles Lactate/ug protein/hr
Vector
Flag 3
***
***
0
1
2
3
4
6
24
Time Span (hr)

D

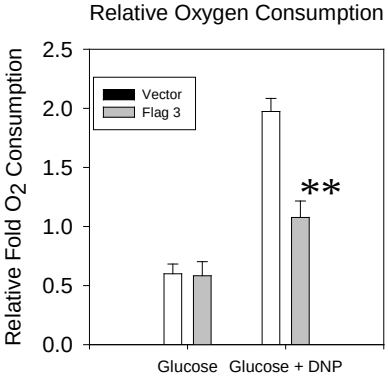
Relative Oxygen Consumption
Relative Fold O2 Consumption
Vector
Flag 3
**
0.0
0.5
1.0
1.5
2.0
2.5
Glucose
Glucose + DNP

E

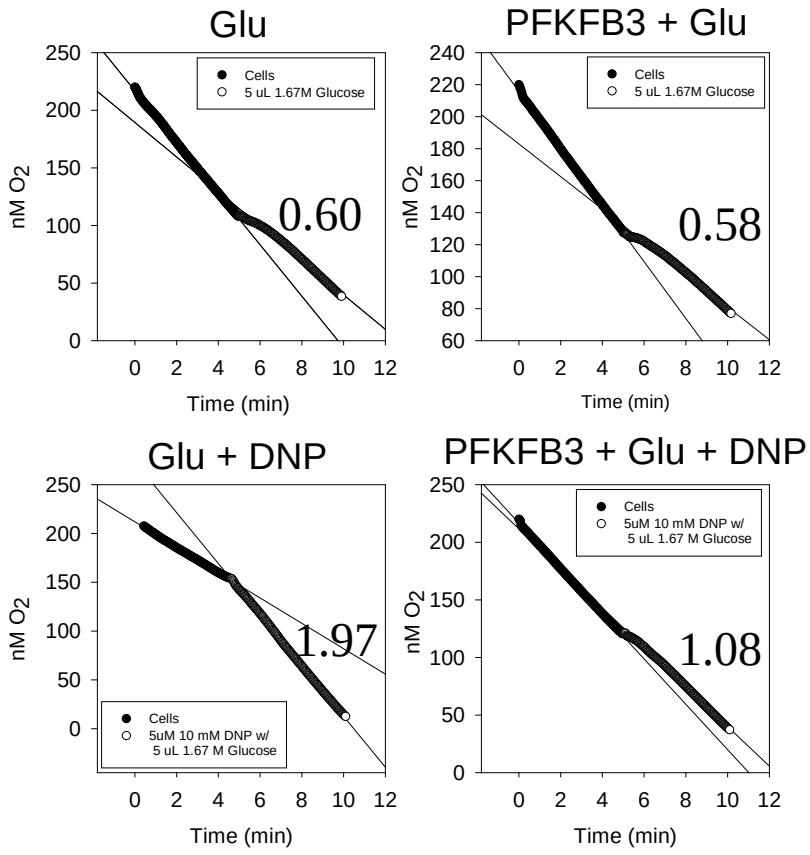

Figure 3.2. Effect of PFKFB3 expression on glycolysis and oxygen consumption. (A) Characterization of PFKFB3 overexpression in DB-1 cells and the effect on rate of (B) glucose consumption, (C) lactate production and (D) oxygen consumption with and without DNP. (E) Representative Clark Electrode oxygen consumption readings, numbers indicate relative rate post addition (post treatment rate/pretreatment rate). Bars are Mean $\pm$ SE of three independent experiments. ** $p < 0.01$-0.001, *** $p < 0.001$ when compared to control.

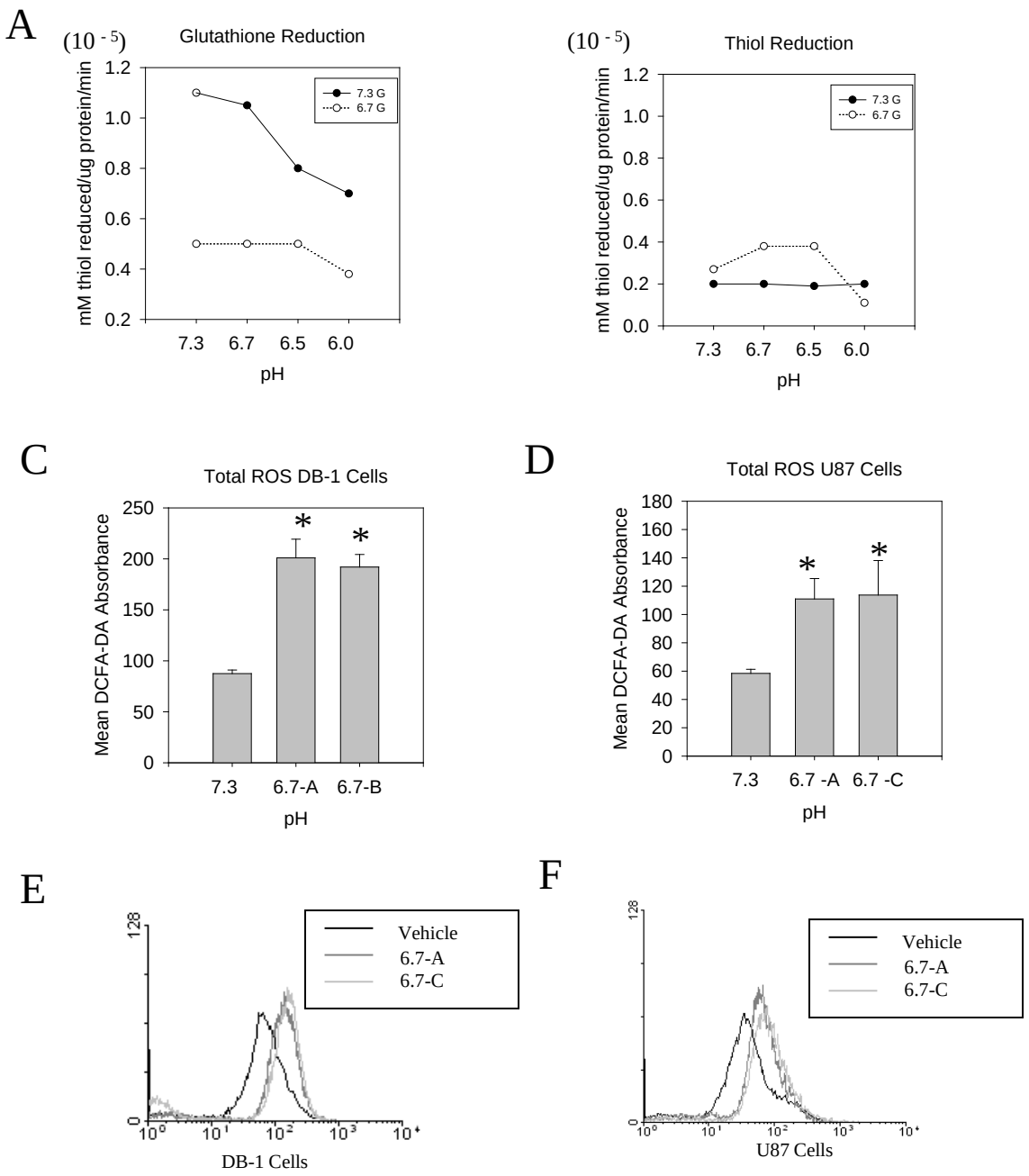

Figure 3.3. Impact of pH on bioreduction capacity and ROS production. Rate of glutathione reduction measured by (A) HEDS bioreduction and thioredoxin activity measured by (B) lipoate bioreduction and total ROS production measured by DCFA-DA staining in (C,E) DB-1 Cells. Total ROS production measured by DCFA-DA staining in (D, F) U87 cells. Bars are Mean $\pm$ SE of three independent experiments. * $p < 0.05$ when compared to control.

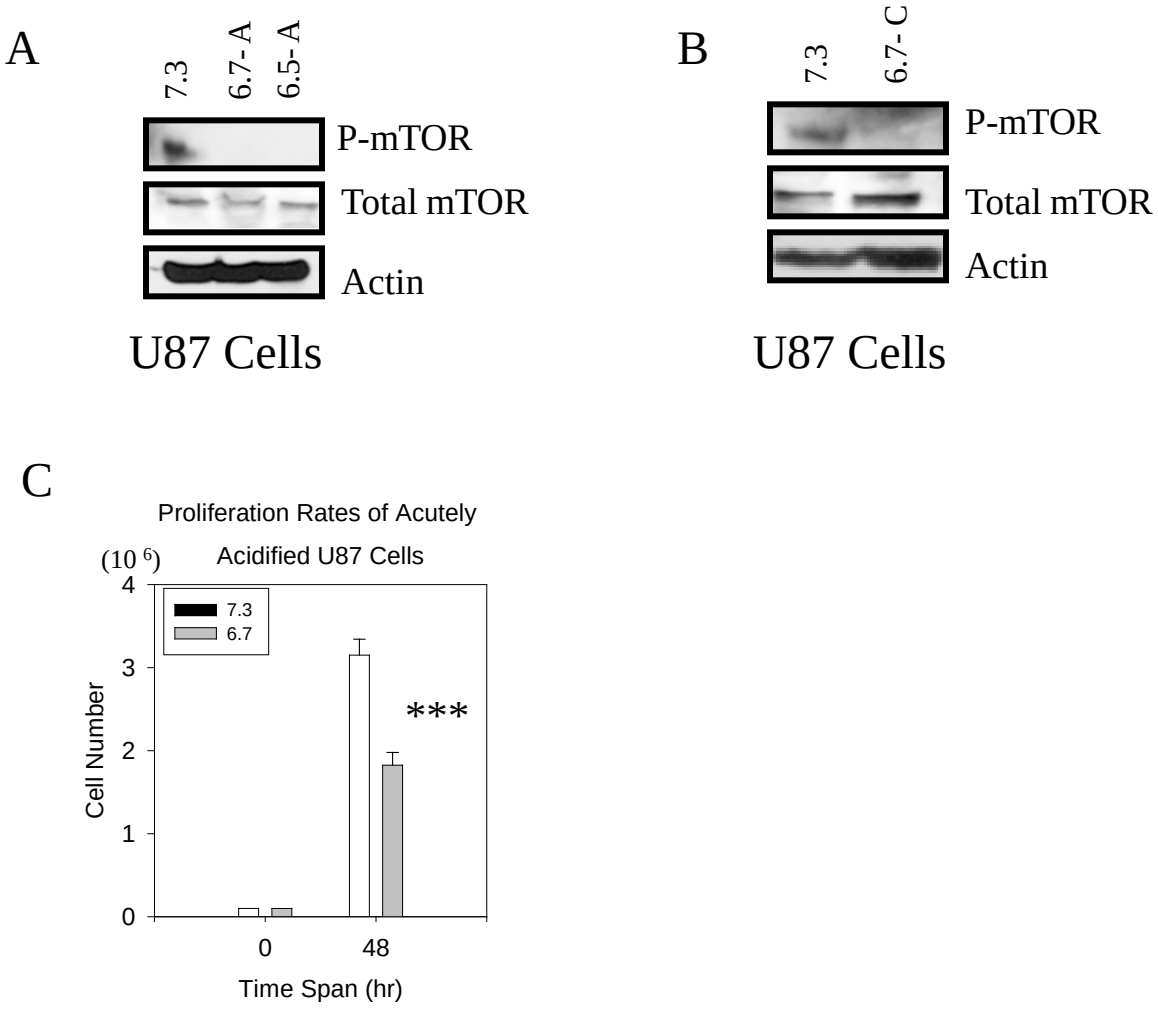

Figure 3. 4. Effect of pH on mTOR expression and cellular proliferation in U87 cells. Western blot of total and phosphorylated mTOR in (A) acutely and (B) chronically acidified cells and the effect of acidification on (C) rates of proliferation. Bars are Mean $\pm$ SD of representative experiment in triplicate samples. * $p < 0.05$ when compared to control. Experiment was repeated three times.

A

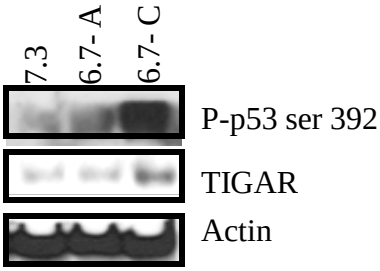

DB-1 Cells

B

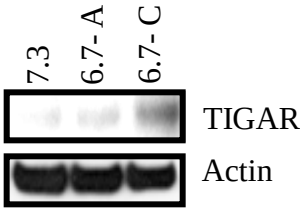

U87 Cells

C

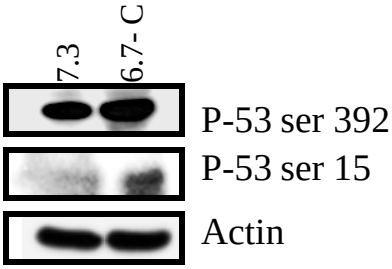

U87 Cells

D

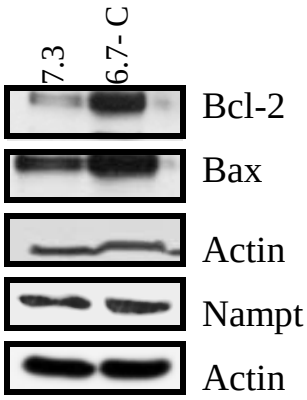

U87 Cells

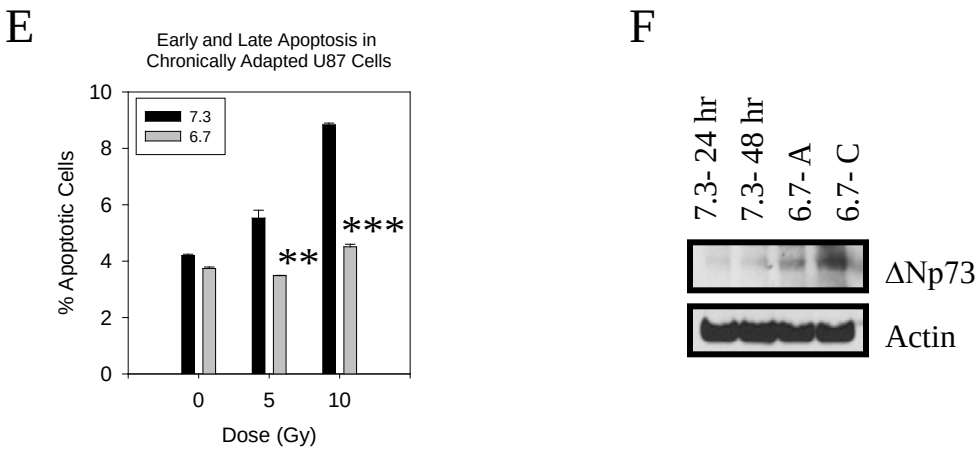

Figure 3.5. Expression of p53 and p53-dependent proteins and impact of pH on apoptosis. Western blot of (A) phosphorylated p53 ser 392 and TIGAR in DB-1 and U87 (B) acutely and (C) chronically acidified cells. (D) Western blot of phosphorylated p53 ser 392 and ser 15, Bcl-2, Bax, and Nampt. (E) Quantification of early and late apoptosis measured by Annexin/FITC staining in chronically acidified U87 cells. (F) Induction of the p53 antagonist ΔNp73 in chronically acidified DB-1cells.

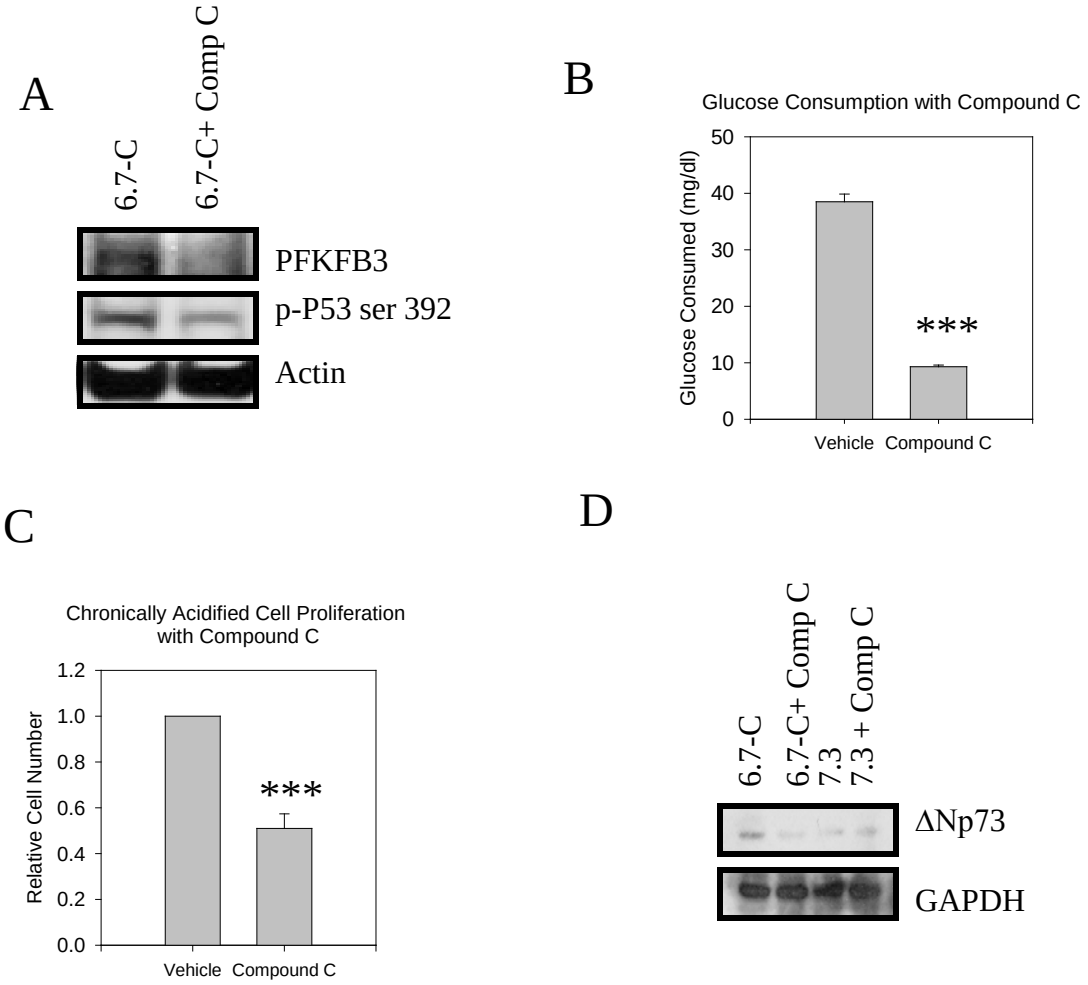

Figure 3.6. Inhibition of AMPK decreases PFKFB3 expression and glycolysis. Western blot of (A) PFKFB3 and p53 in chronically acidified U87 cells. (B) Rate of glycolysis in U87 after 8 hour treatment with Compound C. (C) Cell number 72 hours after treatment with Compound C. (D) Inhibition of ΔNp73 induction in DB-1 cells following treatment with Compound C Bars are Mean $\pm$ SE. *** $p < 0.001$ when compared to control. Experiments in this figure were repeated twice.

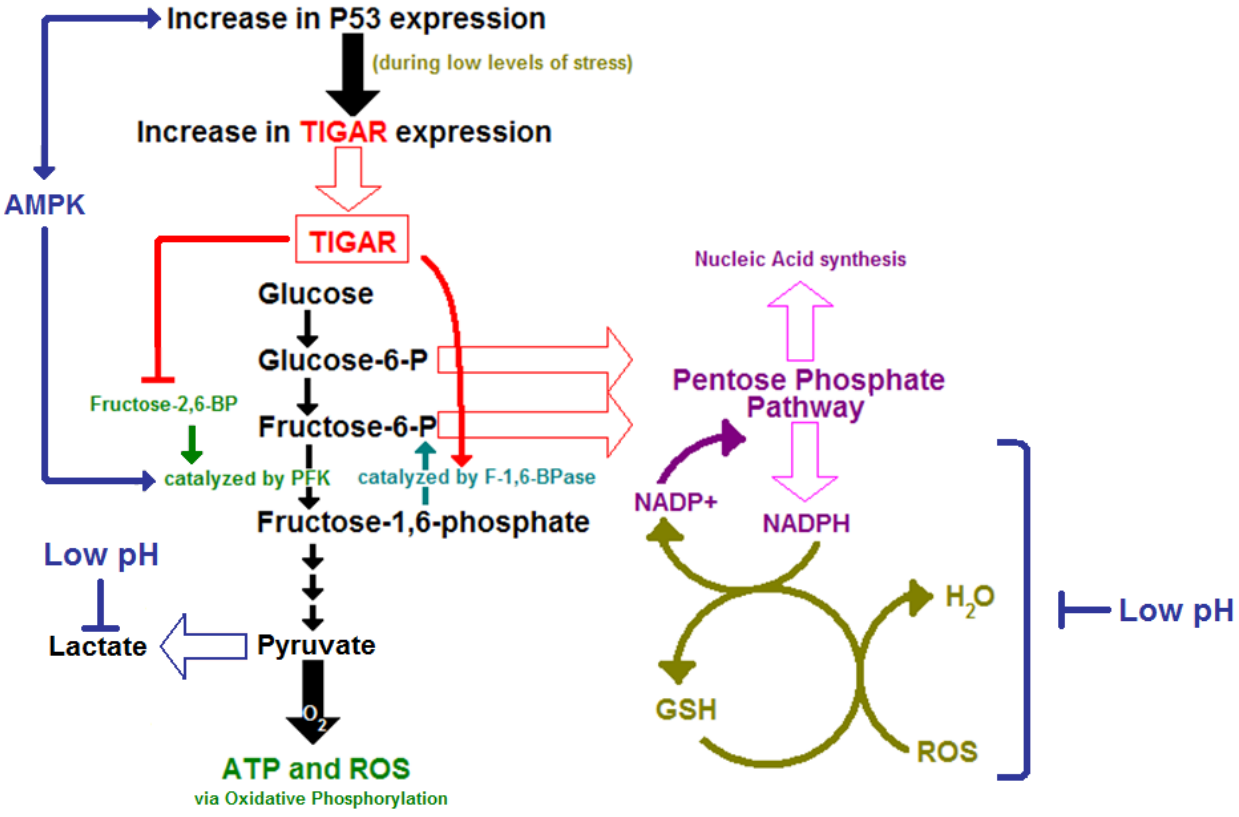

Schematic 3.1

CHAPTER IV: MAINTENANCE OF P53 HOMEOSTASIS IN TUMOR CELLS BY RIBOFLAVIN-STIMULATED NQO1 BINDING ACTIVITY

Abstract

Riboflavin is phosphorylated by flavokinase to create flavin mononucleotide (FMN), which is then adenylated by flavin adenine dinucleotide (FAD) synthetase into FAD. FMN and FAD are required as coenzymes in numerous REDOX reactions, including NQO1-mediated reactions. In addition to its role as a two electron reductase, NQO1 also has protein stabilizing properties and has been shown to stabilize the tumor suppressor p53. Tumor cells can quickly become depleted of riboflavin by the upregulation of export proteins such as Breast Cancer Resistance Protein (BCRP). It was therefore hypothesized that changes in riboflavin levels could alter NQO1 activity and affect its protein stabilizing activities. These results demonstrate that high dose supplementation with riboflavin increased NQO1 activity, while depletion of riboflavin reduced it. The activity of NQO1 caused binding and stabilization of p53 as determined by co-immunopreciatation. Depletion of riboflavin had a negative effect on p53 stability and decreased its association with NQO1. Apoptosis was increased with supplementation, and depletion followed by supplementation resulted in a large increase in apoptosis. Treatment of cell lystates with a flavokinase inhibitor, cadmium, also decreased p53 binding to NQO1. In low pH-adapted cells which were shown to have high NQO1 activity and rely on p53 as a transcription factor, depletion of riboflavin resulted in cell death. Therefore, tumor cells at normal pH depleted of riboflavin could

be sensitized to apoptosis by supplementation of riboflavin; while a riboflavin antagonist would likely target low- pH adapted cells. The results presented here demonstrate for the first time the importance of riboflavin in p53 homeostasis. Tumor cells can quickly become depleted of riboflavin by the upregulation of export proteins such as BCRP.

Introduction

Riboflavin is a quinone-containing compound with electron transfer capabilities. It is widely used as a cofactor in many reactions. To become an active cofactor, riboflavin goes through multiple enzymatic steps; being converted to FMN and ultimately FAD, which is facilitated by flavokinase. Although riboflavin is in considerable excess in many cell types and tissues, studies have shown that riboflavin can be quickly depleted by elimination of the multidrug resistant BCRP. Very few studies have considered the effect of riboflavin depletion on tumor cell metabolism or growth.

NQO1 is a bioreductive enzyme involved in many two-electron reduction reactions. The holoenzyme utilizes riboflavin as a cofactor in all of its bioreductive reactions. Riboflavin acts as an electron intermediate using electrons donated from NAD(P)H. In addition to its bioreductive properties, it also binds many proteins such as p53. Asher et al has shown that NQO1 activity is essential for p53 stability and prevention of degradation (Asher et. al., 2002a). The mechanism appears to be mediated by the binding of NQO1 to p53, preventing proteosomal degredation and MDM2 binding interference (Asher et. al., 2002b). Cells with mutant NQO1 have a higher rate of malignancy (Begleiter et. al., 2006), which further provides evidence that NQO1-mediated p53 stability could play an important role in tumorigenesis.

It has been proposed in patients with reduced NQO1 capability that reduced enzyme capacity could be improved by supplementation (Ames et. al., 2002). This raises the possibility that supplementation or treatment with riboflavin agonists could improve p53 function in depleted tumor cells. This could be particularly useful in tumor cells of the

breast where BCRP is upregulated. Therefore, investigating the effects of riboflavin NQO1 activity and p53 stability could prove to be clinically important.

This report describes for the first time that supplementation of riboflavin increases p53 stability through NQO1 binding, while depletion of riboflavin decreases NQO1 activity and its affinity for p53. We have proposed a novel role for riboflavin as a mediator of NQO1- p53 binding, consequently underscoring its importance in p53 stabilization and homeostasis.

Materials and Methods

Cell Culture

Early passage U87 glioblastoma cells were grown as monolayers at 37° C in humidified 5% CO2 in α-MEM medium supplemented with 10% FBS, 12 mM glucose, 10 mL/L nonessential amino acids solution, and 2.9 g/L glutamine (α-MEM+). Low pH medium was prepared at pH 6.7 as described (Burd et. al., 2001). Cells were grown at pH 7.3 or grown at low pH conditions at pH 6.7. The 6.7 grown cells were adapted to growth at pH 6.7 for at least 14 days, but no more than 60 days before they were used in experiments. Acute acidification was for 48 hours. Depletion experiments were conducted using custom riboflavin deplete α-MEM (Hyclone Thermo Scientific).

Western blotting

Cells grown in culture were washed twice with cold PBS and lysed with LDS sample buffer containing DTT added just prior to use. Buffer also contained aprotinin, AEBSF, sodium orthovanadate, and sodium fluoride to prevent degredation by proteases and phosphatases. Western blotting was carried out with a total of 25 μg as quantified by Protein Dotmetrics kit (Applied Biosystems). Samples were run using 7% or 10% NUPAGE gels (Invitrogen Corp., CA, USA) using a Novex protein standard (Invitrogen). The proteins were transferred onto polyvinylidene difluoride membranes (Amersham Pharmacia Biotech, Piscataway, NJ). Western detection was carried out using CDP star from Tropix, Applied Biosystems (Chicago, IL, USA). Primary antibody to p-p53 ser 392 (Cell Signaling Technologies) was used at a dilution of 1:1,000 and NQO1 (Abcam) was

used at a dilution of 1:10,000. Primary antibodies to Actin (Sigma) and GAPDH (Santa Cruz Biotechnologies) were used at a dilution of 1:10,000.

RNA isolation and real-time Reverse-Transcript Polymerase Chain Reaction (RT-PCR)

Homogenization of cells and isolation of RNA were performed using QIA shredder spin columns and an RNeasy Kit as instructed by the manufacturer (Qiagen, Valencia, CA, USA). 1 μg of RNA was reverse transcribed using a Super Script III Kit as instructed by the manufacturer (Invitrogen, Carlsbad, CA, USA) and diluted 1:5 for subsequent analyses. The following real-time reaction mix was prepared: 5 μl of diluted cDNA, 1 μl of mixed forward and reverse primers (10 μM each), 12.5 μl of SYBR Green (Qiagen), and nuclease-free water to a final volume of 25 μl. All real time RT-PCRs were run in triplicate for each cDNA sample using an iQ5 RT-PCR Detection System (BioRad, Hercules, CA, USA). Forty cycles of PCR were performed (95°C for 15seconds, 54°C for 30 seconds, 72°C for 30 seconds); fluorescence detection occurred during the 72°C step at each cycle. The data were analyzed using the 2-ΔΔCt method (Gallagher et. al., 2003) and results were normalized to S15, which remains unchanged in response to treatment. Normalized values were plotted as relative fold over untreated. The following primers were purchased from Integrated DNA Technologies (Coralville, IA, USA): S15, Bax, and NQO1.

Annexin V-FITC staining

After treatment, adhered cell monolayers were trypsinized and washed twice with

cold PBS. Apoptosis was determined using Annexin V-FITC apoptosis detection kit (R&D systems, MN, USA) as per manufacturer's instructions. 5 × 105 cells were resuspended in 100 µl of 1× binding buffer and mixed with 1 µl of Annexin V-FITC and 10 µl of propidium iodide. After 15 min incubation in the dark at room temperature, 400 µl of 1× binding buffer was added and the cells were analyzed using a BD FACS flow cytometer.

NQO1 Enzymatic Assay

Protocol for measurement of NQO1 activity was adapted from Ernster et al. (Ernster et. al., 1962). Cells were grown in culture and NQO1 activity was inhibited with 400 µM dicoumarol for 4 hr. Adhered monolayers were washed twice with cold PBS and then lysed with .05% Triton-X containing protease inhibitor cocktail added immediately before used. Cells were put through 3 rapid freeze thaw cycles and the insoluble fraction was removed by centrifugation. Lysates were treated with 20 µM riboflavin for 1 hr at 4°C on a rotating platform. Standard reaction mixture contained 77 µM cytochrome c (Sigma), 200 µM NADH (Sigma), 10 µM menadione (Sigma), 0.14% BSA (Sigma); all dissolved in 50 mM tris HCL adjusted to pH 7.5. Assay was measured using a kinetic protocol on an ULTRAMARK BioRad Imaging Microplate System at 550 nm at 25 °C.

Cellular Proliferation Assay

Cells grown in 6-well culture plates were trypsinized and pelleted via

centrifugation, then counted using a hemocytometer following trypan blue staining. Only viable cells were counted and used in cell number analysis.

Immunoprecipiations

Following treatment, cells grown in culture were washed twice with ice cold PBS and then were lysed with ice cold NP-40 buffer substituted with 1% Triton X, 150 mM NaCl, and 50 mM tris HCL. Protease inhibitor cocktail, NaF, and NaV were added immediately before use. Lysates were immunoprecipitated with 4µl anti-NQO1 antibody overnight at 4°C with gentle agitation. Lysates were then incubated with 50 µl Protein G bead slurry (Sigma) for 1 hr at 4°C on a rocking platform. Beads were then pelleted by centrifugation and washed three times with buffer. LDS sample buffer was then added to beads and samples boiled for 10 min at 100 °C, and supernatant was removed.

Results

NQO1 is a two-electron reductase that binds and stabilizes other proteins and complexes. The bioreduction processes mediated by NQO1 require riboflavin as electron transfer intermediate and NAD(P)H as an electron source. We therefore investigated the effect of riboflavin on NQO1 activity. Treatment of cell lysates with riboflavin increased NQO1 activity by 2-fold (Figure 4.1A). Asher et. al. (2004) has demonstrated that NQO1 binds and stabilizes p53, which increases p53's function as a pro-apoptotic molecule. We therefore investigated if riboflavin supplementation could enhance binding. The addition of 20 μM riboflavin increased the association of phosphorylated p53 serine 392 (p-p53 ser 393) with NQO1 (Figure 4.1B), while other phosphorylated species were not detected. FAD serves as an essential cofactor for NQO1, and FAD is derived from dietary riboflavin, with flavokinase as the rate-limiting enzyme. Addition of a flavokinase inhibitor, cadmium sulfate, resulted in a decreased affinity of p-p53 ser 392 (Figure 4.1C). Real time RT-PCR demonstrated that a transcription of NQO1 was unaffected by riboflavin treatment (Figure 4.1 D).

Stabilization of p53 is a way for cells to increase its levels (Asher, 2002). Therefore we determined protein levels following supplementation with riboflavin. Western blot analysis indicated that p-p53 ser 392 was induced following 12 or 24 hour incubation with 20μm riboflavin (Figure 4.2 A). Total p53 was also increased and indicated riboflavin contributed to p53 stabilization. The increased pro-apoptotic p53 was also associated with an increase in caspase and PARP cleavage (Figure 4.2 B). A minor increase in apoptosis was also observed following treatment (Figure 4.2C),

coinciding with the increase in p53 and cleavage of intrinsic apoptotic proteins. The pro-apoptotic protein Bax was observed to have increased transcription measured by quantitative RT-PCR and confirmed a pro-apoptotic environment and p53 transcriptional activity (Figure 4.2D).

To demonstrate that the induction of p53 is not through the induction of DNA damage but rather stabilization of NQO1, we investigated the effect of riboflavin on p-ATM which is phosphorylated after DNA damage (Figure 4.3A). Following 4 hr treatment with 200 μM dicoumarol, a known ROS inducer and NQO1 inhibitor, an induction of phosphorylation of ATM was observed, indicating a DNA damage response. Dual treatment with both dicoumarol and riboflavin decreased ATM activation, indicating a restoration of NQO1 bioreductive capacity.

To determine if p53 activity could be restored, riboflavin was added back at increasing concentrations. Levels of p-p53 ser 392 increased dose dependently up to 60 μm (Figure 4.4B). This increase was associated with a large increase in apoptosis (Figure 4.4C). The levels of apoptosis increased significantly and were greater than supplementation alone (Figure 4.2).

We have previously shown that cells adapted to growth at low pH have elevated levels of p53 (See Chapter 3).We hypothesized that the induction of p53 could be due to an increase in NQO1 activity resulting from adaptation to the electrophillic low-pH environment. As shown in Figure 4.5A, cells grown at pH 6.7 had a ~1.4 fold increase in NQO1 activity. Correspondingly there was an increase in p53 and NQO1 (Figure 4.5B). In contrast to other tumor cells, the induction of p53 in low-pH adapted cells is

crucial to their survival as p53 acts as an important transcription factor of glycolytic proteins (See Chapter 3). Decreasing p53 in low-pH adapted cells resulted in cell death in a p53-independent manner (Figure 3.6). Because of the importance of p53 in these cells, we tested the effect of riboflavin depletion on survival, p53 was decreased following depletion and resulted in selective cell death of low-pH cells (Figure 5C).

Discussion

Riboflavin is phosphorylated by flavokinase to create flavin mononucleotide (FMN), which is then adenylated by flavin adenine dinucleotide (FAD) synthetase into FAD. FMN and FAD are required as coenzymes in numerous REDOX reactions, including NQO1-mediated reactions. We have demonstrated that high dose supplementation with riboflavin can increase the activity of NQO1, while depletion reduces activity. The activity of NQO1 was associated with the binding and stabilization of p53. These results were consistent with Asher et. al. (2006) who showed NQO1 stabilizes p53 (Asher et. al., 2004). Furthermore, it was reported that mutations in NQO1 could decrease its activity and binding to p53, further reducing p53 stability (Begleiter et. al., 2009). Studies in colon cancer cells indicated that mutations in NQO1 can increase carcinogenesis (Begleiter et. al., 2006). It has been proposed that cofactor supplementation in patients with mutant NQO1 can increase its activity and restore the wildtype phenotype (Ames et. al., 2002). The results presented here support the notion that NQO1 function can be abrogated by riboflavin concentration. The concentration for supplementation used here is not physiological, but in conjunction with the depletion studies argue that sufficient riboflavin concentrations are required for proper p53 homeostasis. It has been demonstrated that tumor cells can become depleted of riboflavin in 4 days (van Herwaarden et. al., 2007). This would likely reduce p53 stability and render cells less sensitive to apoptosis.

Because p53 is important in protection from tumorigenesis, the study of p53 stabilization is important. In addition to MDM2 degradation, p53 is degraded by 20S

proteasomes (Asher et. al., 2002b; Sollner and Macheroux, 2009). The degradation of p53 via 20S is independent of ubiquitination (Gong et. al., 2007). It has also been demonstrated that cytosolic NQO1 and NQO2 protect p53 from 20S proteasomal degradation. In addition, overexpression of NQO1 and NQO2 stabilize p53, potentially by blocking the binding of p53 to the 20S proteosome (Gong et. al., 2007). As demonstrated by the immunoprecipitation data, our results support the conclusion that low NQO1 activity via cadmium inhibition can reduce the affinity of p53 for NQO1.

Radiation for example is potentiated by the presence of apoptosis (Gimenez-Bonafe et. al., 2009) and the absence of p53 would be another means of tumor escape in cells that were riboflavin deficient (Gimenez-Bonafe et. al., 2009). Tumor cells can become depleted of riboflavin by the up regulation of the multi-drug resistance protein BCRP. This protein has been shown to be upregulated in tumors, and therefore its inhibition presents a viable target.

In the case of the low pH adapted cells we have previously demonstrated that p53 is important because it induces TIGAR and deltaNp73 (See Chapter 3). These two proteins would protect cells from glycolysis-induced acidification and apoptosis (Bensaad et. al., 2006; Melino et. al., 2002; Thoreen and Sabatini, 2005). NQO1 has also been shown to stabilize the full-length p73 (Asher et. al., 2005). Therefore it is highly probable that the deletion mutants of p73 which have p53 antagonist properties could also be stabilized. These cells were sensitive to non-p53 mediated death following riboflavin depletion, which further confirms the central role of p53 as a transcription factor (Figure 4.5 D). This supports other observations, which describe alterations in transcription

factor activity modulated by riboflavin, and indicates that riboflavin antagonists may have an important role in anti-tumor therapies.

The results presented here for the first time demonstrate the importance of riboflavin in p53 homeostasis. Depletion of riboflavin had a major effect on p53 stability and its association with NQO1. In low pH adapted cells, which rely on p53 as a transcription factor, riboflavin depletion resulted in cell death. Therefore, tumor cells depleted of riboflavin could be sensitized to apoptosis by supplementation of riboflavin, while riboflavin antagonist would likely target low pH adapted cells.

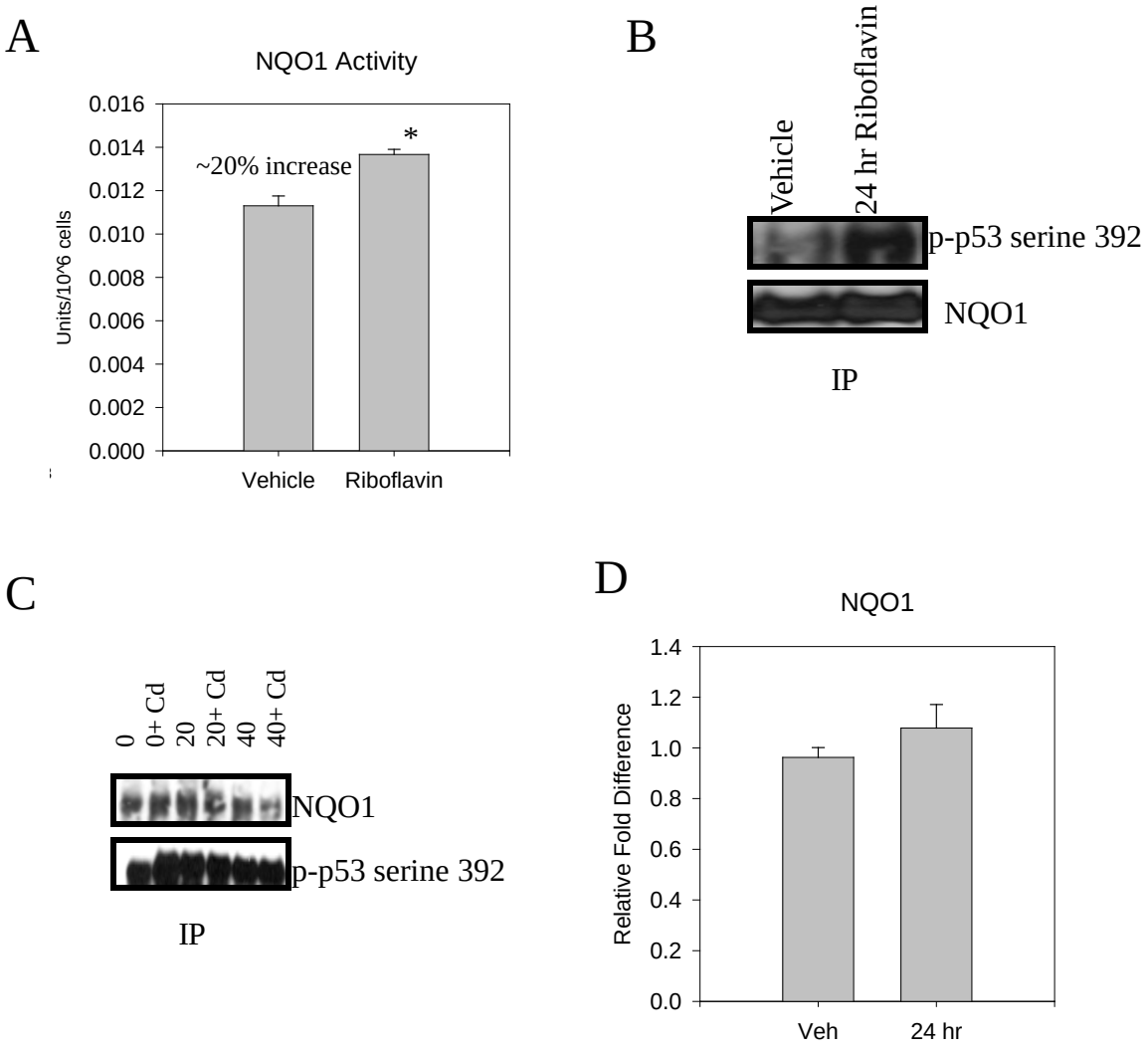

Fig 4.1. Riboflavin increases NQO1 activity and affinity of NQO1 and p53 binding post-transcriptionally. (A) Measurement of NQO1 activity and (B) immunoprecipitation of NQO1 and western blot p-p53 ser 392 following 24 hr 20 μM riboflavin treatment. Immunoprecipiation of NQO1 and western blot with and without treatment with 100μM cadmium sulfate to inhibit flavokinase (C). Quantification of NQO1transciptional activity using RT-PCR (D). Mean ± SE. mRNA levels not statistically different from control. Experiments in this figure were repeated twice.

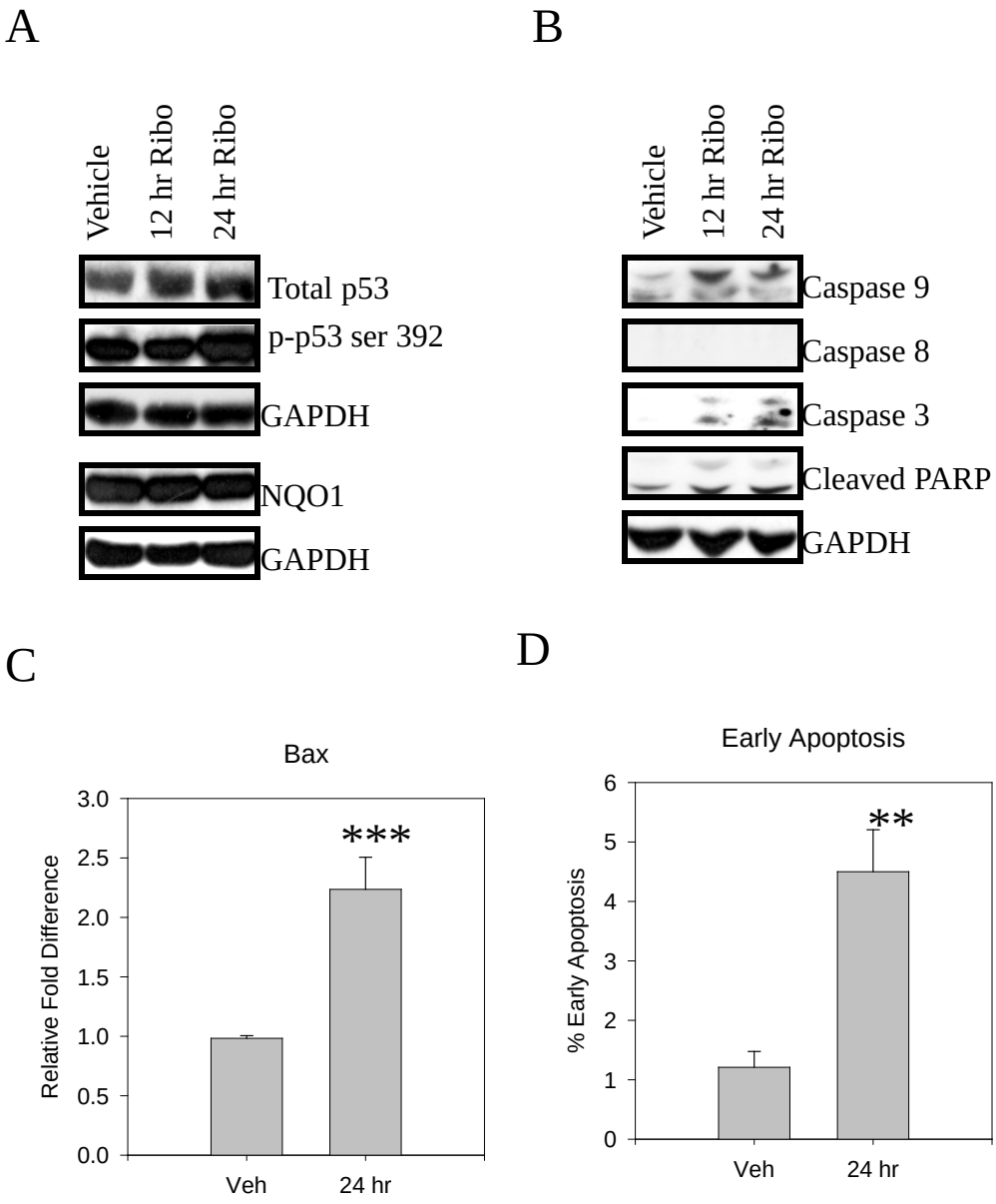

Figure 4.2. Riboflavin treatment increases p53 expression and induces a pro-apoptotic environment. Western blot of total and phosphorylated p53 ser 392 and NQO1 following 12 and 24 hr 20 μM riboflavin treatment (A) and (B) caspase 9, 8, 3, and PARP cleavage. (C) Quantification of Bax transcriptional activity using RT-PCR and (D) analysis of early apoptosis using Annexin V staining following 24 hr 20μM riboflavin treatment. Bars are Mean $\pm$ SD of representative experiment in triplicate samples. ** $p < 0.01$-0.001 and *** $p < 0.001$ when compared to control. Experiment was repeated three times.

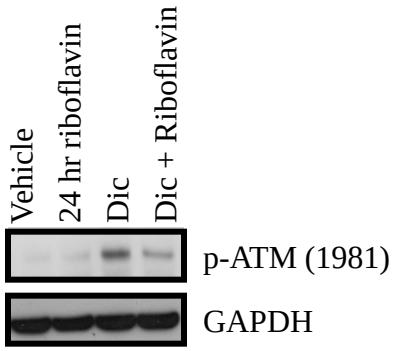

Figure 4.3. Riboflavin does not induce DNA damage response. Western blot of total and phosphorylated ATM following treatment with 20 μM riboflavin, 4 hr 200 μM dicoumarol, or a combination (A). Experiment was repeated twice.

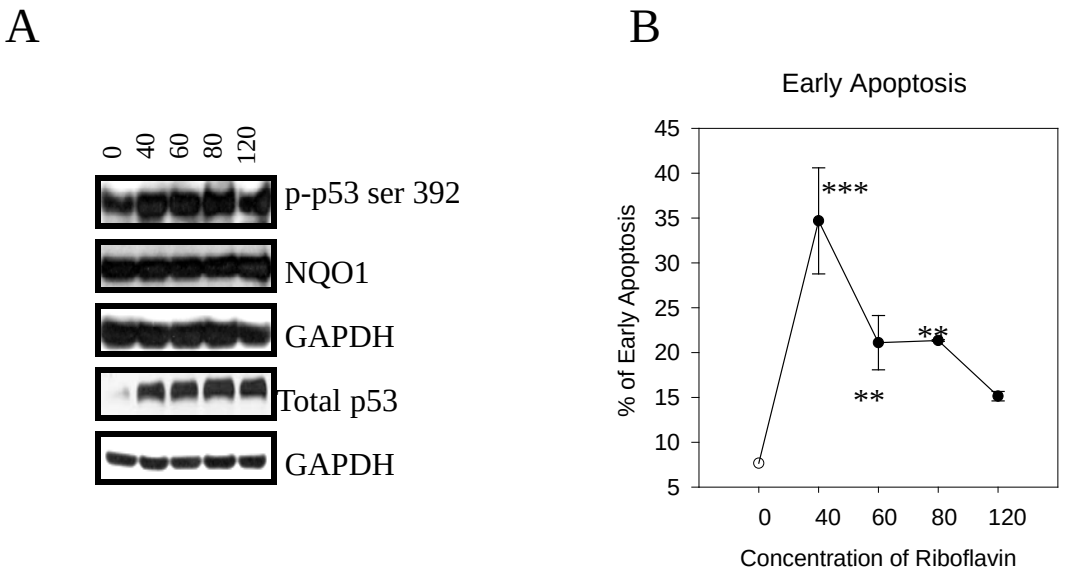

Figure 4.4. Riboflavin depletion leads to p53 destabilization and re-supplementation restores activity and pro-apoptotic environment. Western blot of total and phosphorylated p53 ser 392 and NQO1 (A) and (B) analysis of early apoptosis using Annexin V staining following following a 24 hr dose escalation riboflavin treatment following 24 hr riboflavin depletion. Bars are Mean $\pm$ SD of representative experiment in triplicate samples. ** $p < 0.01$-0.001 *** $p < 0.001$ when compared to control. Experiment was repeated three times.

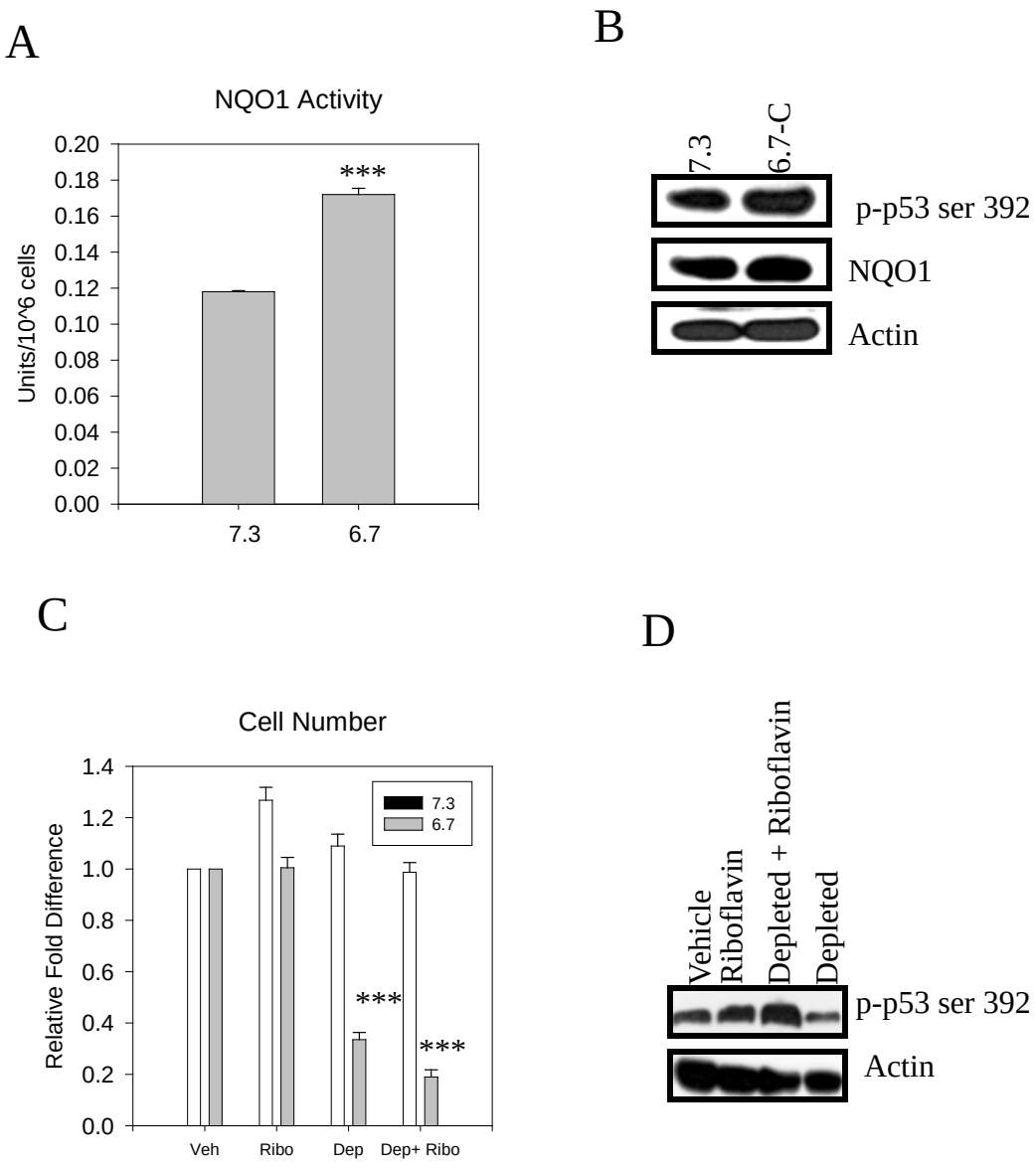

Figure 4.5. NQO1 enzymatic activity is increased and riboflavin depletion leads to selective cell death in chronically acidified cells. (A) Measurement of NQO1 enzymatic activity and (B) western blot of total and phosphorylated p53 ser 392 and NQO1 in 7.3 cells versus chronically acidified cells. (C) Cell number and (D) western blot of p-p53 ser 392 following either treatment with 20 μM riboflavin for 24 hrs, riboflavin depletion for 24 hrs, or a combination Bars are Mean $\pm$ SD of representative experiment in triplicate samples. *** $p < 0.001$ when compared to control. Experiment was repeated three times.

CHAPTER V: ENHANCEMENT OF RADIATION RESPONSE BY EXPLOITING THE HYPOXIC TUMOR MICROENVIRONMENT

Abstract

Bioreductive drugs are bioreduced by intracellular reductases into active DNA damaging moieties and may selectively sensitize hypoxic tumor cells. This would complement therapeutic radiation because hypoxia can induce significant radiation resistance. The bioreductive enzyme profile, specifically the ratio of two: one electron reductases or NAD(P)H quinone oxidoreductase1(NQO1):Cytochrome P450 reductase (cp450r) has a major impact on hypoxic selectivity. A high ratio of NQO1:cp450r would favor cytoxicity in oxygenated cells, while a low ratio would favor toxicity in hypoxic cells. Therefore, the effect of tumor hypoxia on the bioreductive ezyme profile and bioreductive drug toxicity was investigated. U87 human glioblastoma cells were treated with hypoxia (2% oxygen) or hypoxia mimetics. Tumors were also grown subcutaneously in the hind limb of athymic NCR NUDE mice and allowed to grow to a hypoxic volume of $\approx$500 mm^3 before treatment. EO9 (3 days X 2 mg/kg) or vehicle (DMSO) was administered 30 min after each radiation fraction (3 days x 7.5 Gy) on day 1, 2, and 3. Hypoxia decreased NQO1 and the ratio of NQO1:cp450r in tumor cells and xenografts. Radiation therapy further elevated the levels of cp450r. Combination treatment of EO9 and radiotherapy increased tumor growth delay (TGD) greater than a comparable regimen of EO9 alone ($p<0.001$), or radiation alone ($p=0.027$ comparing days 1-7). These results indicate that EO9 can benefit a fractionated regimen of radiotherapy and should be explored clinically as a radiation sensitizer. Furthermore,

hypoxia and radiation can alter the bioreductive enzyme profile and favor hypoxic cell kill by bioreductive drugs. Future studies will address optimal scheduling of EO9 with radiation as well as systemic delivery of EO9 in combination with radiation therapy.

Introduction

Radiation therapy is an effective modality for the treatment of a number of tumors. Half of all cancer patients will receive radiation therapy during their course of treatment. While radiation therapy is one of the most widely used treatments for cancer, many tumors are hypoxic and subsequently resistant to radiation therapy (Owen et. al., 1992). Therefore, there remains a need to improve therapeutic outcome of radiation therapy, especially in hypoxic tumors. One way to enhance the effectiveness of radiation therapy is to use a radiation sensitizer, a drug that increases the effectiveness of radiation without sensitizing normal tissue.

Hypoxic cell sensitizers are quinone compounds that rely on bioreductive enzymes in tumors to become activated. Apaziquone (EO9) is a novel analogue of Mitomycin C that has the potential to act as a radiosensitizer (Bailey et. al., 1998; Cummings et. al., 1998; Loadman et. al., 2002). EO9 is bioreduced by intracellular reductases into active DNA damaging moieties(Bailey et. al., 1998) and may selectively target hypoxic cells. The reductases expressed in tumors may play an important role in the selectivity of EO9. NQO1 (NAD(P)H quinone oxidoreductase1), a two electron reductase, may selectively target oxygenated cells, while enzymes catalyzing one electron reduction such as Cytochrome P450 reductase (cp40r) may be more effective in targeting hypoxic cells (Spanswick et. al., 1998).

Ongoing clinical trials investigating EO9 in superficial bladder tumors with local drug delivery show promising response rates with minimal normal tissue toxicity (Jain et. al., 2009). However, the effect of a combination of EO9 with radiation has not been fully

investigated. The purpose of this study was to explore the effect of hypoxia on the enzyme. EO9 can be used as a radiation sensitizer because of the potential of EO9 to damage DNA and selectively target hypoxic cells with minimal damage to normal tissue.

Materials and Methods

Animal and tumor models

U87 glioblastoma cells (American Type Culture Collection) were maintained in alpha MEM medium (Sigma) with 10% fetal bovine serum (Atlanta Biologicals). A U-87 cell suspension was injected subcutaneously into the right hind limb (5×10^5 cells in 100 μl PBS) of athymic NCR NUDE mice (Taconic Farms).

Tumor oxygen measurements

Tumor oxygen tension was measured using the Oxford Oxylite fiberoptic probe (Oxford, England). The detection system is based on blue light excitation of ruthenium pigment at the end of a fiber optic probe, which is quenched by oxygen. Measurements were performed on anesthetized mice (75 mg/kg Ketamine and 0.3 mg/kg Acepromazine), while body temperature was maintained at 37°C with a heating pad. A 25 gauge needle was used to puncture the tumor capsule to facilitate insertion of the fiberoptic probe. The probe was guided into the tumor at a 2-4 mm depth.

Tumor growth delay

U87 human glioblastoma cells were injected subcutaneously into the right hind limb of athymic NCR NUDE mice and allowed to grow to a hypoxic volume of ~550 mm^3 before treatment. EO9 or vehicle was administered 30 min. after each radiation fraction on day 1, 2, and 3. The study used 4 treatment groups: vehicle (DMSO),

radiation alone (3 days x 7.5 Gy), EO9 (3 days x 2 mg/kg), and EO9 + radiation. EO9 was administered locally by intra-tumoral injection to achieve optimal delivery.

Tumor growth statistics

Mixed–effects regression was used to model the base-10 logarithm of tumor volume as a function of time and treatment (tumor growth analyses). The log-transformed outcome was used because tumors of this size grow approximately exponentially, and therefore the logarithm of the tumor volume is approximately linear over time. This approach appropriately handles unbalanced data, such as a different number of measurements for different animals, and takes into account the correlation of each animal's measurements over time. These analyses were carried out with SAS 8.2 (SAS Institute Inc., Cary, NC, 1999-2001).

Western Blot analysis

Samples were resolved on NuPage 10% bis-Tris gels (Invitrogen, Carlsbad, CA). The proteins were transferred onto polyvinylidene difluoride membranes (Amersham Pharmacia Biotech, Piscataway, NJ) using a semidry transfer apparatus (Pharmacia-LKB multiphor II). Immunoblotting was performed with monoclonal and polyclonal antibodies: anti-human NQO1, anti-human Cytochrome P450 reductase and anti-GAPDH. Immunodetection was performed by enhanced chemiluminescence using a Tropix Western-Star protein detection kit (Applied Biosystems; Foster City, CA).

Results

The ratio of NQO1:cp450r is important for bioreductive drugs which are activated after they undergo one or two electron reduction. Because hypoxic cells are the target of bioreductive drugs we investigated the effect of the hypoxic microenvironment on enzyme profiles. In U87 cells exposed to 2% oxygen, NQO1 was reduced in a time dependent manner after 24 and 48 hr (Figure 5.1A) of exposure to hypoxia. The levels of cp450r were not consistently changed by hypoxia (Figure 5.1A) and were minimally increased by hypoxia mimmetics (Figure 5.1B). Because radiation therapy is commonly used in conjunction with bioreductive drugs we investigated the effect of ionizing radiation on bioreductive enzymes. Cp450r was increased by a single fraction of 7.5 Gy (single fraction size used for U87 xenografts) (Figure 5.1C). NQO1 was induced in a dose dependent manner (Figure 5.1C).

The tumor suppressor p53 plays an important role in bioreductive drug toxicity and has an important role in p53 stabilization. We investigated the impact of hypoxia on p53. Hypoxia decreased NQO1 in a time dependent manner and p53 decreased correspondingly at 16 and 24 hrs, but increased after 48 hrs (Figure 5.2A). Hypoxia mimetics had a similar destabilizing effect, decreasing both p53 and NQO1 at 24 hrs (Figure 5.2B).

We next investigated the effect of tumor volume on hypoxia in U87 tumor xenografts. Tumors were grown to differing volumes and then tumor oxygen tension was measured. As tumors increased in size the median oxygen tension decreased from 253 to 5 mmHg (Figure 5.3). Tumors were then removed and western blot analysis was used to

determine tumor enzyme profile. As tumor volume and hypoxia increased, the ratio of NQO1:cp450r decreased (Figure 5.4). We also confirmed the effect of radiation therapy on on the enzyme ratio. However unlike observed in cell culture, one fraction of radiation to xenografts had no effect on enzyme levels, while 3 fractions of radiation increased levels of cp450r (Figure 5.5). Taken together, these results indicate that hypoxia and radiation affects the range of bioreductive drugs that would be favorable to use as hypoxic cell sensitizers. The high ratio of NQO1:cp450r would favor cytotoxicity in oxygenated cells, while the decrease in the ratio would favor toxicity in hypoxic cells. Radiation would further increase hypoxic sensitivity in radiation resistant hypoxic cells.

To determine the effect of a two electron bioreductive drug on tumor toxicity in hypoxic tumors, U87 xenografts were allowed to grow to hypoxic volumes and treated with radiation and eoquin (EO9) (Figure 5.6). EO9 alone or radiation alone increased tumor-doubling time by 1.4 days ($p<0.001$ vs. control) or 5.2 days ($p<0.001$ vs. control), respectively (Table 5.1). Combination of EO9 and radiotherapy increased the mean doubling time by 8.5 days to 11.7 days, a stronger effect than that seen by a comparable regimen of EO9 alone ($p<0.001$), or radiation alone ($p=0.027$ comparing days 1-7) (Table 5.1). No significant increase in weight loss or normal toxicity was observed in any group after treatment with EO9 (data not shown). These results indicate for the first time that bioreductive drugs can be used to exploit enzymatic profiles induced by hypoxia.

Discussion

Tumors become hypoxic and therefore become resistant to radiation. The enzymes induced however are conducive to the activation of bioreductive drugs, which are introduced as a prodrug to be activated by either one or two electron bioreduction. Induction of these enzymes through radiotherapy could implicate bioreductive drugs as a beneficial adjuvant therapy to radiation alone. However, the radiation doses used in this study are substantially lower than the fractionated doses used clinically, and may not lead to the same induction of the enzymatic profile needed to potentiate bioreductive drug activation and should be studied further.

Hypoxia selectivity serves as the primary purpose for making the incorporation of bioreductive drugs a part of routine therapy. Hypoxic tissues showing an increase in cp450r would have a therapeutic advantage to selectively activate prodrugs to the active form, while preventing auto-oxidation back to the parent compound. The presence of oxygen coupled with a down regulation of cp450r would render the drug inactive in normal tissues, decreasing toxicity. Clinical studies show that EO9 targets tumor tissue in bladder with little normal tissue toxicity (Jain et. al., 2009). These tumors have also been shown to be hypoxic and support the results presented here (Ioachim et. al., 2006).

The interaction of p53 and NQO1 leads to stabilization and prevention of proteasomal degradation (Asher, 2005). The early decrease in p53 observed with hypoxia as well as the hypoxia mimetic DMOG, which prevents Hif-1 degradation, was associated with a decrease in NQO1. This observation potentially rules out acidification as the inhibitor of NQO1 because the cells treated with the mimetic were maintained at a

normal pH. The increase in p53 seen after 48 hours of hypoxia was likely a result of cell death and an increase in ROS. Decreasing NQO1 can induce futile ROS cycling and has been shown to increase ROS and p53 (nkova-Kostova and Talalay, 2010). Levels of p53 were elevated in tumor cells *in vitro* and therefore p53 levels should also be measured in tumors. However, in bladder tumors and glioma where bioreductive drugs would likely be used, p53 is either mutated (Cordon-Cardo, 2008) or offset by high levels of DNA repair (Zhang et. al., 2010).

The mechanism of NQO1 down regulation is unclear, but likely involves Hif-1 activation because the hypoxia mimetic also caused downregulation of NQO1 and rules out acid effects. A similar down regulation of NQO1and its family members by hypoxia mimetic have previously been shown (Davidson et. al., 2003). It was demonstrated that the Aryl Hydrocarbon genes, which are related to NQO1, were also decreased by the induction of Hif-1. The downregulation was attributed to alterations in iron metabolism resulting from inhibition of hydroxylases (Davidson et. al., 2003). Others demonstrate that Hif-1 can bind p53, which may affect NQO1's association and its stability (Tsvetkov et. al., 2010).

Tumor hypoxia is classically associated with an acidic environment, which leads to a significant clinical barrier and an attenuation of weak base chemotherapeutics. In order to comprehensively understand the changes in tumor enzymatic profiles, it is necessary to study the effects of a decreased extracellular pH on enzyme activity. In the acidic microenvironment, conditions favor bioreduction and cells could be sensitized to bioreductive therapies requiring two electron reduction by NQO1. However, we have

shown that acidification upregulates the activity of NQO1. Therefore, the effect of acidification must be examined more closely. Tumor growth delay studies should also be performed in oxygenated cells in order to more closely study drug effects in the oxygenated tumor microenvironment.

Conclusion

These results indicate for the first time that hypoxic cells can induce an enzyme profile that would be optimal for a fractionated regimen of radiotherapy and bioreductive drugs. Future studies will address optimal scheduling of EO9 with radiation as well as systemic delivery of EO9 in combination with radiation therapy. The high ratio of NQO1:cp450r would favor cytotoxicity in oxygenated cells, while the decrease in the ratio would favor toxicity in hypoxic cells. This protocol should be further explored clinically.

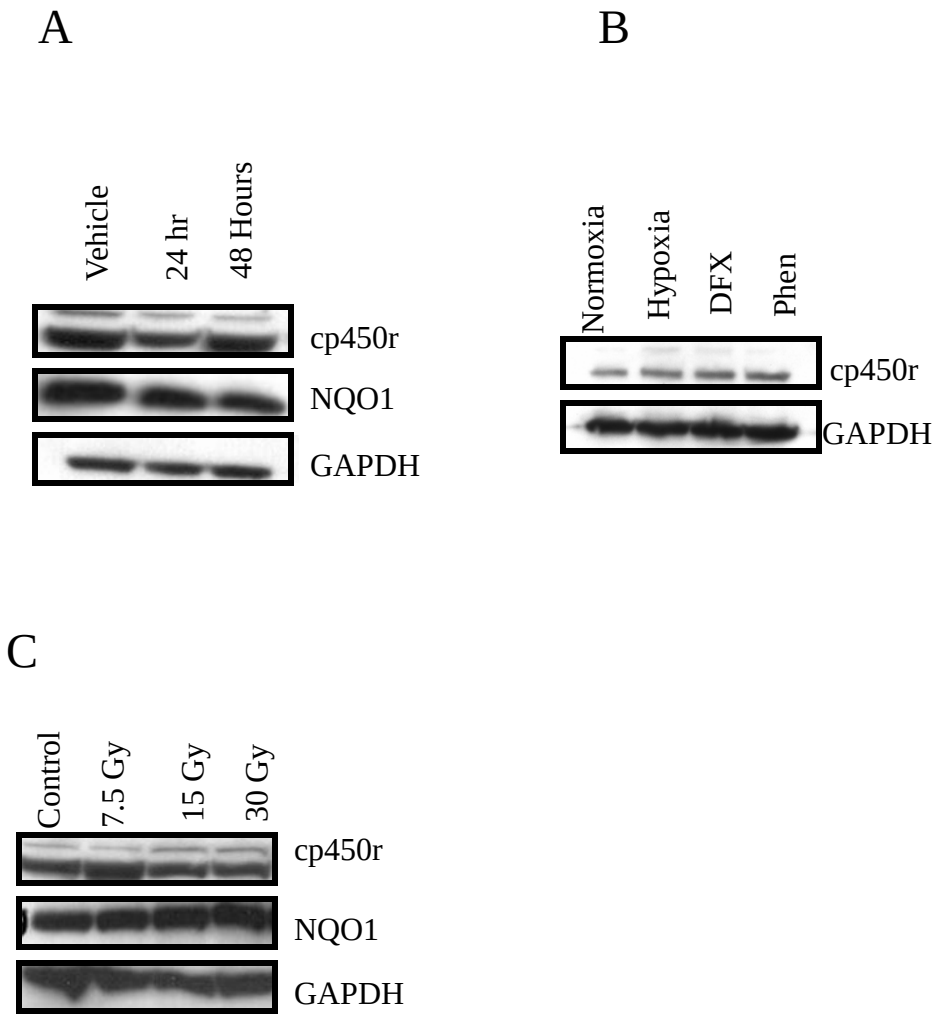

Figure 5.1. Hypoxia and ionizing radiation alter the ratio of NQO1:cp450r in U87 tumor cells. Western blot of normoxic U87 cells and cells treated under hypoxia (2% Oxygen) for increasing hours (A) and then treated with hypoxia mimetic for 24 hrs(B). The ratio of NQO1:cp450r is also affected by ionizing radiation.

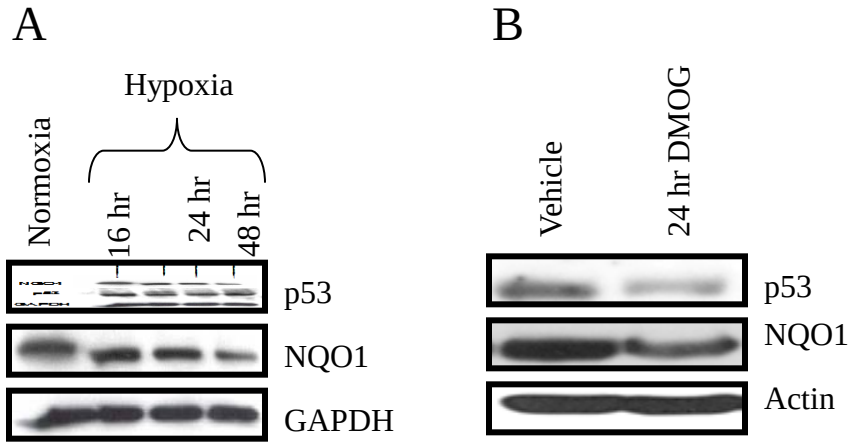

Figure 5.2. Hypoxia downregulates NQO1 and p53 in U87 tumor cells. Western blot of normoxic U87 cells and cells treated under hypoxia for increasing hours (A) and then treated with the hypoxia mimetic DMOG at a concentration of 100 μM for 24 hrs (B).

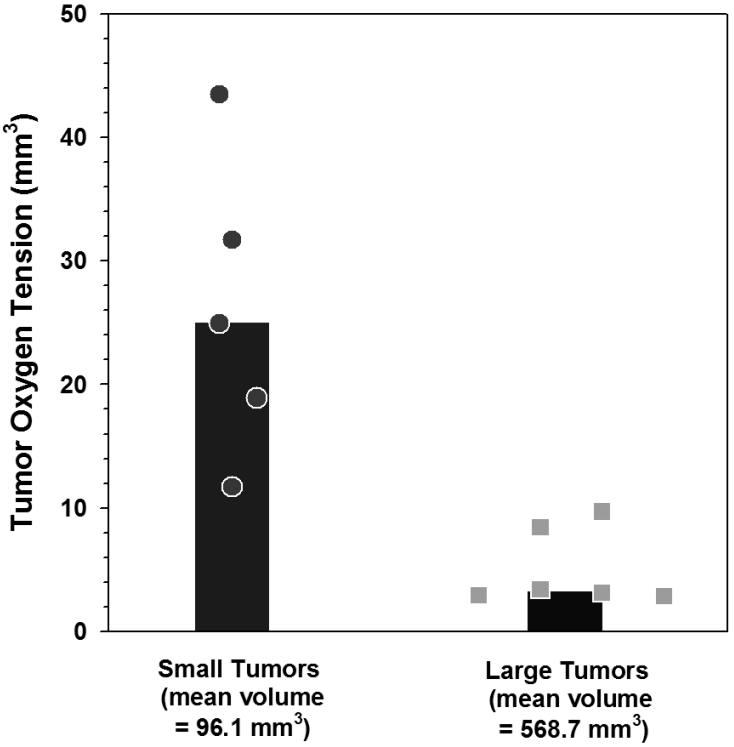

Figure 5.3. Effect of tumor volume on tumor oxygen tension. Shown are the median tumor pO_2 values for multiple small tumors (circles, N=5) and large tumors (squares, N=6). Bars indicate group medians. Tumor oxygen tension was measured using the Oxford Oxylite fiberoptic probe (Oxford, England). A 25 gauge needle was used to puncture the tumor capsule to facilitate insertion of the fiber optic probe. The probe was guided into the tumor at a depth of 2-4 mm.

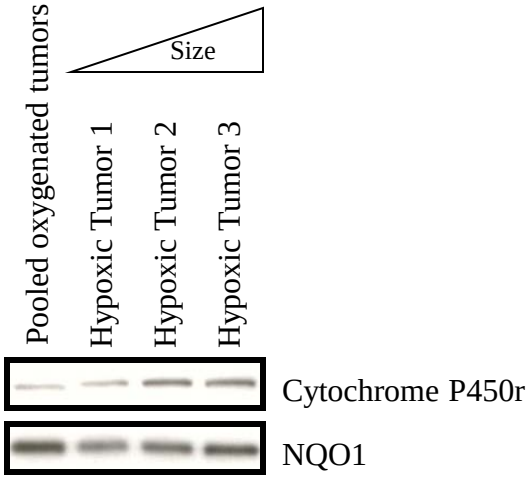

Figure 5.4. Hypoxic tumors have a higher ratio of cp450r:NQO1. Western Blot shows pooled tumor samples(Lane 1) from three small tumors (mean = 143 mm^3), and three hypoxic tumors of increasing size (mean = 693 mm^3).

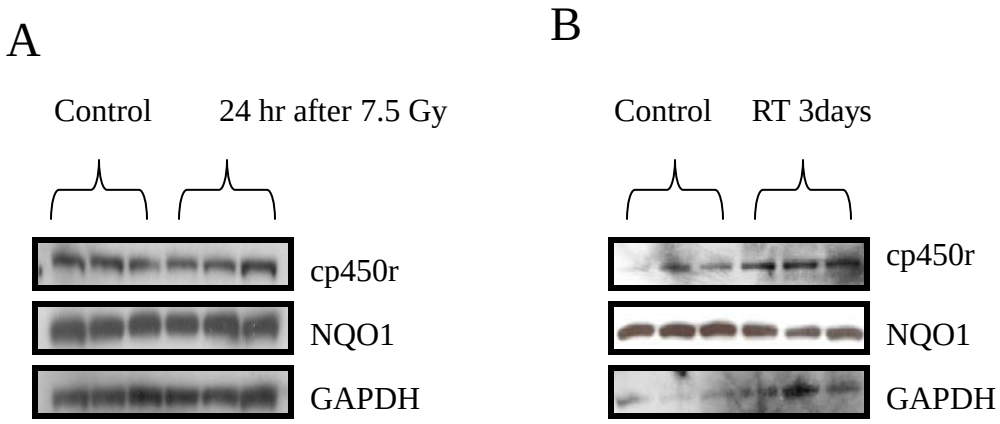

Figure 5.5. Fractionated radiation increases the ratio of cytochrome P450 reductase to NQO1 in tumor xenografts. Western Blot shows three different untreated tumors (Control 1, 2, 3) and three tumors (RT 1, 2, 3) that were irradiated with three daily fractions of 7.5 Gy. Samples were harvested 24 hrs. after last irradiation.

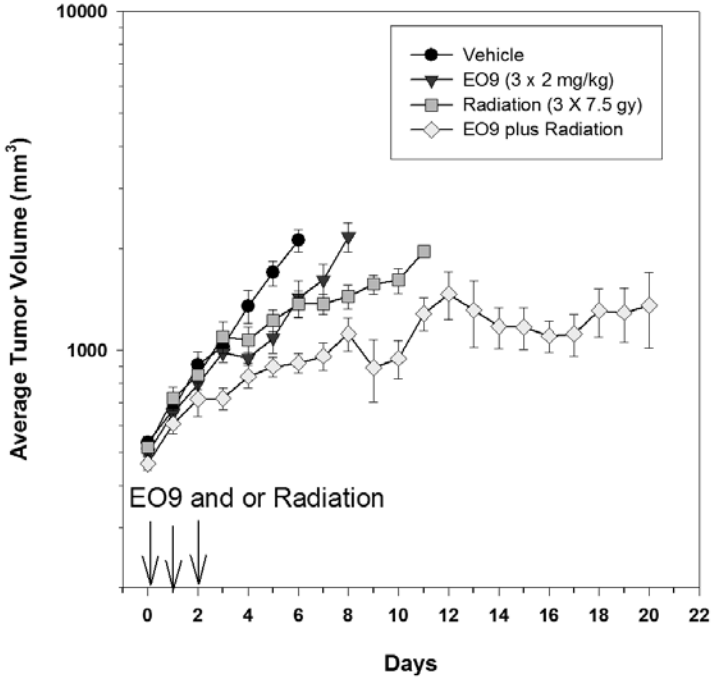

Figure 5.6. Mean and SE for EO9 or vehicle administered 30 min. after radiation on day 0, 1, and 2. The study used 4 treatment groups: vehicle (DMSO), radiation alone (3 days x 7.5 Gy), EO9 (3 days X 2 mg/kg), and EO9 + radiation. EO9 was administered locally by intra-tumoral injection. All four groups started with similar–sized tumors of ~550 mm^3 ($p = 0.20$ for the comparison of groups at day 0).

Treatment Group	%D (95% CI)		T_{2x}	Time (Days) for tumors to reach 2000 mm^3	p Value
Vehicle	25	(21, 28)	3.2	6.1	
EO9	16	(14, 19)	4.6	8.6	p<0.001 vs. control
RT	9	(6, 11)	8.4	12.7	p<0.001 vs. control
EO9+RT	6	(4, 8)	11.7	20.8	(p<0.001) vs. EO9 alone (p=0.027) vs. RT alone comparing days 1-7

Table 5.1. Estimates of tumor growth rate and doubling time, by treatment group.
% delta (D): average rate of increase of tumor volume (% daily increase).
95% CI: 95% confidence interval.
T2x: average doubling time of tumor volume (in days).

CHAPTER VI: DISCUSSION

Role of p53 in Adaptation to the Tumor Microenvironment

It was hypothesized that the tumor microenvironment would induce signaling and enzymatic changes, manipulated could improve treatment outcome. The results presented here demonstrate that exposure of tumor cells to chronic low pH or hypoxic conditions induced signaling cascades and altered enzyme profiles which resulted in a pro-survival phenotype. Three key adaptation events were observed and included **1)** the up regulation of the metabolic stress and glycolytic kinase AMPK and PFKFB3, respectfully. **2)** The upregulation of p53 and **3)** changes in the ratios of the bioreductive enzymes were also found to be important in the adaptation. P53 was central to the adaptation process because it induced the transcription of anti-glycolytic proteins to control glycolysis and minimize tumor cell acidosis (Figure 6.1).

Upregulation and Activation of AMPK and PFKFB3

The upregulation of AMPK and PFKFB3 play a dominant role in the adaptation process. It was clearly demonstrated that AMPK, a stress response protein was activated and antagonizing AMPK with inhibitors blocked the upregulation downstream of targets, including mTOR and PFKFB3. It was also shown that overexpression of PFKFB3 resulted in the high glycolytic flux that is observed in tumors (Figure 3.2 B). Therefore, PFKFB3 mediated through AMPK could be the trigger for the Warburg Effect. It is also known that tumor cells adapted to low pH must compensate for acid production. Therefore, the upregulation of TIGAR is a plausible mechanism for glycolytic control (Figure 3.5 A-B). P53 could have been upregulated by either AMPK (Thoreen and

Sabatini, 2005) or the induction of ROS. It is also possible that this is a cyclical relationship as p53 can act on AMPK and induce ROS by mitochondrial release of cytochrome c. However, the upregulation of Nampt and inhibition of apoptosis provide evidence that ROS is the result of the reduction in glutathione activity (Figure 6.1). Nonetheless, these results indicate the low pH induces signaling cascades and alters the enzymatic activities of glutathione reductase and support the hypothesis.

Upregulation of p53 by Micronutrients

The micronutrient riboflavin had an effect on p53 homeostasis because increasing NQO1 activity by riboflavin supplementation induced a p53-stabilizing effect by enhancing binding of p53 to NQO1 and protected p53 from degradation. Riboflavin is phosphorylated by flavokinase to create FMN, which is then adenylated by flavin adenine dinucleotide synthetase into FAD. FAD is an important cofactor used by NQO1. We demonstrated that an increase in NQO1 activity enhanced binding to p53. The key experiment supporting the role of NQO1 as a p53 stabilizing molecule was that cadmium, which inhibits flavokinase, caused the dissociation of p53 and NQO1. In the absence of riboflavin there was no further disassociation, indicating that not all p53 is supported by NQO1 activity. Supplementation induced apoptosis, which indicates that riboflavin is important for maintaining p-p53 levels and an active state of p53. The ser 392 p-p53 had the greatest association with NQO1, which is the tetrameric and transcription factor phosphorylation site (Hollstein and Hainaut, 2010; Thoreen and Sabatini, 2005)In low pH-adapted cells which were shown to have high NQO1 activity and rely on p53 as a transcription factor (Figure 4.5 A), depletion of riboflavin resulted in cell death (Figure

4.5 C). Therefore, tumor cells at normal pH depleted of riboflavin could be sensitized to apoptosis by supplementation of riboflavin, while a riboflavin antagonist would likely target low pH adapted cells (Figure 6.1). Therefore, the micronutrient concentration can have substantial effects on p53 status and can co-regulate enzyme activity. Manipulation of this status can also alter the apoptotic response and there for would support the hypothesis that the micronutrient status or manipulation of riboflavin levels can effect survival or therapeutic outcome.

Changes in the Ratios of the Bioreductive Enzymes are Important in the Adaptation and Treatment Response

In addition to the riboflavin effect, it was demonstrated that hypoxia and the potentially associated low pH environment could affect the ratio of NQO1:cp450 reductase. The increase in cytochrome p450 reductase, which is a one electron bioreduction enzyme, has been shown to increase toxicity of bioreductive drugs in hypoxic tumors. NQO1 activity is more important to bioreductive drug sensitization in oxygenated cells. Therefore, the bioreductive state is optimal for bioreductive drug toxicity and will compliment such cytoxic treatment because tumor cells have mixed oxygen states.

A decrease in NQO1 activity could be associated with a decrease in p53. This would work against therapeutic treatment and may possibly be the case in hypoxic and acidic cells (Figure 6.1). However, we did show that the NQO1 stabilizing effect on p53 was not the only pathway for p53 induction, and may play a lesser role to a substantial increase in ROS by the drug or radiation. Taken together, these results indicate that the

changes that occuring in tumor adaptation to the microenvironment require signaling and enzymatic modifications that work together to regulate metabolism and apoptosis. Many of these changes present therapeutic targets that could be exploited to enhance therapy or prevent adaptation and subsequent tumor growth, therefore supporting the hypothesis.

Conclusion

The work presented demonstrates fundamental changes in tumor signaling and enzyme profiles and indicates that multiple pathways work to together to minimize acidification and apoptosis (Figure 6.1). However, the upregulation of these pathways leaves opportunity for exploitation and present viable targets for improved therapy or preventative measures.

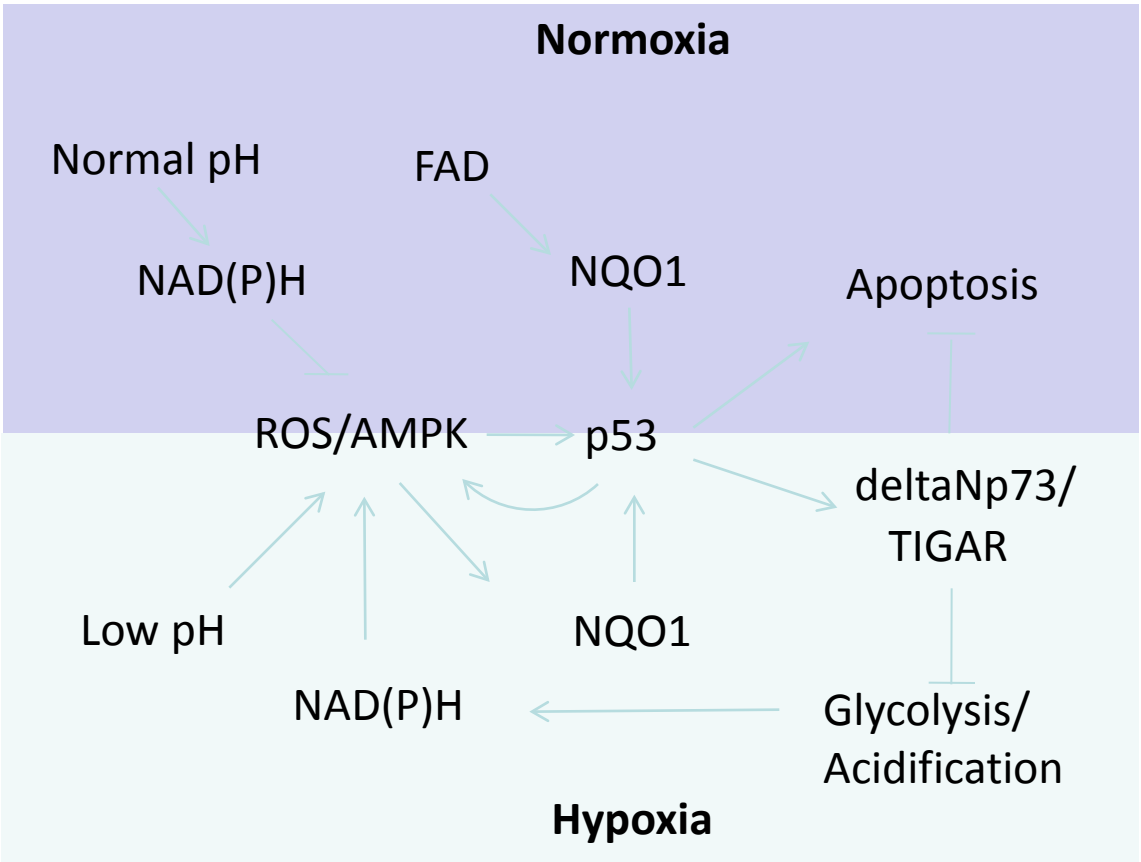

Figure 6.1. Central Role of p53 and ROS in Adaptation. In Normoxic cells glycolysis is maintains NAD(P)H and keeps ROS and AMPK low. NQO1 is minimally supported by FAD. In low pH cells glcolysis is low and therefore ROS and AMPK are elevated, which induces p53. The transcription of TIGAR and p53 antagonists block glyolysis and apoptosis, creating a vicious cycle. Elevated NQO1 activity further maintains p53.

REFERENCES

Ames B.N., Elson-Schwab I., Silver E.A. High-dose vitamin therapy stimulates variant enzymes with decreased coenzyme binding affinity (increased K(m)): relevance to genetic disease and polymorphisms. Am J Clin Nutr 2002;75(4):616-58.

Ansiaux R., Baudelet C., Jordan B.F., Beghein N., Sonveaux P., De W.J., et al. Thalidomide radiosensitizes tumors through early changes in the tumor microenvironment. Clin Cancer Res 2005;11(2 Pt 1):743-50.

Ansiaux R., Baudelet C., Jordan B.F., Crokart N., Martinive P., Dewever J., et al. Mechanism of Reoxygenation after Antiangiogenic Therapy Using SU5416 and Its Importance for Guiding Combined Antitumor Therapy. Cancer Res 2006;66(19):9698-704.

Asher G., Lotem J., Kama R., Sachs L., Shaul Y. NQO1 stabilizes p53 through a distinct pathway. Proc Natl Acad Sci U S A 2002a;99(5):3099-104.

Asher G., Lotem J., Sachs L., Kahana C., Shaul Y. Mdm-2 and ubiquitin-independent p53 proteasomal degradation regulated by NQO1. Proc Natl Acad Sci U S A 2002b;99(20):13125-30.

Asher G., Lotem J., Sachs L., Shaul Y. p53-dependent apoptosis and NAD(P)H:quinone oxidoreductase 1. Methods Enzymol 2004;382:278-93.

Asher G., Tsvetkov P., Kahana C., Shaul Y. A mechanism of ubiquitin-independent proteasomal degradation of the tumor suppressors p53 and p73. Genes Dev 2005;19(3):316-21.

Atsumi T., Chesney J., Metz C., Leng L., Donnelly S., Makita Z., et al. High expression of inducible 6-phosphofructo-2-kinase/fructose-2,6-bisphosphatase (iPFK-2; PFKFB3) in human cancers. Cancer Res 2002;62(20):5881-7.

Bailey S.M., Lewis A.D., Knox R.J., Patterson L.H., Fisher G.R., Workman P. Reduction of the indoloquinone anticancer drug EO9 by purified DT-diaphorase: a detailed kinetic study and analysis of metabolites. Biochem Pharmacol 1998;56(5):613-21.

Bao S., Wu Q., McLendon R.E., Hao Y., Shi Q., Hjelmeland A.B., et al. Glioma stem cells promote radioresistance by preferential activation of the DNA damage response. Nature 2006;444(7120):756-60.

Beall H.D., Winski S.I. Mechanisms of action of quinone-containing alkylating agents. I: NQO1-directed drug development. Front Biosci 2000;5:D639-D648.

Begleiter A., Hewitt D., Maksymiuk A.W., Ross D.A., Bird R.P. A NAD(P)H:quinone oxidoreductase 1 polymorphism is a risk factor for human colon cancer. Cancer Epidemiol Biomarkers Prev 2006;15(12):2422-6.

Begleiter A., Sivananthan K., Lefas G.M., Maksymiuk A.W., Bird R.P. Inhibition of colon carcinogenesis by post-initiation induction of NQO1 in Sprague-Dawley rats. Oncol Rep 2009;21(6):1559-65.

Bensaad K., Cheung E.C., Vousden K.H. Modulation of intracellular ROS levels by TIGAR controls autophagy. EMBO J 2009;28(19):3015-26.

Bensaad K., Tsuruta A., Selak M.A., Vidal M.N., Nakano K., Bartrons R., et al. TIGAR, a p53-inducible regulator of glycolysis and apoptosis. Cell 2006;126(1):107-20.

Biaglow J.E., Donahue J., Tuttle S., Held K., Chrestensen C., Mieyal J. A method for measuring disulfide reduction by cultured mammalian cells: relative contributions of glutathione-dependent and glutathione-independent mechanisms. Anal Biochem 2000;281(1):77-86.

Bohensky J., Terkhorn S.P., Freeman T.A., Adams C.S., Garcia J.A., Shapiro I.M., et al. Regulation of autophagy in human and murine cartilage: hypoxia-inducible factor 2 suppresses chondrocyte autophagy. Arthritis Rheum 2009;60(5):1406-15.

Boyle R.G., Travers S. Hypoxia: targeting the tumour. Anticancer Agents Med Chem 2006;6(4):281-6.

Burd R., Lavorgna S.N., Daskalakis C., Wachsberger P.R., Wahl M.L., Biaglow J.E., et al. Tumor oxygenation and acidification are increased in melanoma xenografts after exposure to hyperglycemia and meta-iodo-benzylguanidine. Radiat Res 2003;159(3):328-35.

Burd R., Wachsberger P.R., Biaglow J.E., Wahl M.L., Lee I., Leeper D.B. Absence of Crabtree effect in human melanoma cells adapted to growth at low pH: reversal by respiratory inhibitors. Cancer Res 2001;61(14):5630-5.

Chan N., Koch C.J., Bristow R.G. Tumor hypoxia as a modifier of DNA strand break and cross-link repair. Curr Mol Med 2009;9(4):401-10.

Chesney J., Mitchell R., Benigni F., Bacher M., Spiegel L., Al-Abed Y., et al. An inducible gene product for 6-phosphofructo-2-kinase with an AU-rich instability element: role in tumor cell glycolysis and the Warburg effect. Proc Natl Acad Sci U S A 1999;96(6):3047-52.

Cordon-Cardo C. Molecular alterations associated with bladder cancer initiation and progression. Scand J Urol Nephrol Suppl 2008;(218):154-65.

Cummings J., Spanswick V.J., Gardiner J., Ritchie A., Smyth J.F. Pharmacological and biochemical determinants of the antitumour activity of the indoloquinone EO9. Biochem Pharmacol 1998;55(3):253-60.

Danson S., Ward T.H., Butler J., Ranson M. DT-diaphorase: a target for new anticancer drugs. Cancer Treat Rev 2004;30(5):437-49.

Davids L.M., Kleemann B., Cooper S., Kidson S.H. Melanomas display increased cytoprotection to hypericin-mediated cytotoxicity through the induction of autophagy. Cell Biol Int 2009;33(10):1065-72.

Davidson T., Salnikow K., Costa M. Hypoxia inducible factor-1 alpha-independent suppression of aryl hydrocarbon receptor-regulated genes by nickel. Mol Pharmacol 2003b;64(6):1485-93.

de M.A., Canese R., Marino M.L., Borghi M., Iero M., Villa A., et al. pH-dependent antitumor activity of proton pump inhibitors against human melanoma is mediated by inhibition of tumor acidity. Int J Cancer 2009.

Di C.G., Hatazawa J., Katz D.A., Rizzoli H.V., De Michele D.J. Glucose utilization by intracranial meningiomas as an index of tumor aggressivity and probability of recurrence: a PET study. Radiology 1987;164(2):521-6.

Drakos E., Atsaves V., Li J., Leventaki V., Andreeff M., Medeiros L.J., et al. Stabilization and activation of p53 downregulates mTOR signaling through AMPK in mantle cell lymphoma. Leukemia 2009;23(4):784-90.

Dvorak H.F. Vascular permeability factor/vascular endothelial growth factor: a critical cytokine in tumor angiogenesis and a potential target for diagnosis and therapy. J Clin Oncol 2002;20(21):4368-80.

Ernster L., DANIELSON L., LJUNGGREN M. DT diaphorase. I. Purification from the soluble fraction of rat-liver cytoplasm, and properties. Biochim Biophys Acta 1962;58:171-88.

Fang J.S., Gillies R.D., Gatenby R.A. Adaptation to hypoxia and acidosis in carcinogenesis and tumor progression. Semin Cancer Biol 2008;18(5):330-7.

Ferrara N., Gerber H.P., LeCouter J. The biology of VEGF and its receptors. Nat Med 2003;9(6):669-76.

Fukumura D., Jain R.K. Tumor microvasculature and microenvironment: targets for anti-angiogenesis and normalization. Microvasc Res 2007;74(2-3):72-84.

Fukumura D., Xu L., Chen Y., Gohongi T., Seed B., Jain R.K. Hypoxia and acidosis independently up-regulate vascular endothelial growth factor transcription in brain tumors in vivo. Cancer Res 2001;61(16):6020-4.

Gallagher R.E., Yeap B.Y., Bi W., Livak K.J., Beaubier N., Rao S., et al. Quantitative real-time RT-PCR analysis of PML-RAR alpha mRNA in acute promyelocytic leukemia: assessment of prognostic significance in adult patients from intergroup protocol 0129. Blood 2003;101(7):2521-8.

Gatenby R.A., Gawlinski E.T., Gmitro A.F., Kaylor B., Gillies R.J. Acid-mediated tumor invasion: a multidisciplinary study. Cancer Res 2006;66(10):5216-23.

Gatenby R.A., Gillies R.J. Why do cancers have high aerobic glycolysis? Nat Rev Cancer 2004;4(11):891-9.

Gillies R.J., Gatenby R.A. Adaptive landscapes and emergent phenotypes: why do cancers have high glycolysis? J Bioenerg Biomembr 2007b;39(3):251-7.

Gillies R.J., Gatenby R.A. Hypoxia and adaptive landscapes in the evolution of carcinogenesis. Cancer Metastasis Rev 2007a;26(2):311-7.

Gimenez-Bonafe P., Tortosa A., Perez-Tomas R. Overcoming drug resistance by enhancing apoptosis of tumor cells. Curr Cancer Drug Targets 2009;9(3):320-40.

Gong X., Kole L., Iskander K., Jaiswal A.K. NRH:quinone oxidoreductase 2 and NAD(P)H:quinone oxidoreductase 1 protect tumor suppressor p53 against 20s proteasomal degradation leading to stabilization and activation of p53. Cancer Res 2007;67(11):5380-8.

Gorski D.H., Beckett M.A., Jaskowiak N.T., Calvin D.P., Mauceri H.J., Salloum R.M., et al. Blockage of the vascular endothelial growth factor stress response increases the antitumor effects of ionizing radiation. Cancer Res 1999;59(14):3374-8.

Hague A., Bracey T.S., Hicks D.J., Reed J.C., Paraskeva C. Decreased levels of p26-Bcl-2, but not p30 phosphorylated Bcl-2, precede TGFbeta1-induced apoptosis in colorectal adenoma cells. Carcinogenesis 1998;19(9):1691-5.

Hollstein M., Hainaut P. Massively regulated genes: the example of TP53. J Pathol 2010;220(2):164-73.

Huber P.E., Bischof M., Jenne J., Heiland S., Peschke P., Saffrich R., et al. Trimodal cancer treatment: beneficial effects of combined antiangiogenesis, radiation, and chemotherapy. Cancer Res 2005;65(9):3643-55.

Inai T., Mancuso M., Hashizume H., Baffert F., Haskell A., Baluk P., et al. Inhibition of vascular endothelial growth factor (VEGF) signaling in cancer causes loss of endothelial fenestrations, regression of tumor vessels, and appearance of basement membrane ghosts. Am J Pathol 2004;165(1):35-52.

Ioachim E., Michael M., Salmas M., Michael M.M., Stavropoulos N.E., Malamou-Mitsi V. Hypoxia-inducible factors HIF-1alpha and HIF-2alpha expression in bladder cancer and their associations with other angiogenesis-related proteins. Urol Int 2006;77(3):255-63.

Izumi Y., Xu L., di T.E., Fukumura D., Jain R.K. Tumour biology: herceptin acts as an anti-angiogenic cocktail. Nature 2002;416(6878):279-80.

Jain A., Phillips R.M., Scally A.J., Lenaz G., Beer M., Puri R. Response of multiple recurrent TaT1 bladder cancer to intravesical apaziquone (EO9): comparative analysis of tumor recurrence rates. Urology 2009;73(5):1083-6.

Jain R.K. Molecular regulation of vessel maturation. Nat Med 2003;9(6):685-93.

Jain R.K. Normalization of tumor vasculature: an emerging concept in antiangiogenic therapy. Science 2005;307(5706):58-62.

Jain R.K. Normalizing tumor vasculature with anti-angiogenic therapy: a new paradigm for combination therapy. Nat Med 2001;7(9):987-9.

Koh M.Y., Spivak-Kroizman T.R., Powis G. HIF-1alpha and cancer therapy. Recent Results Cancer Res 2010;180:15-34.

Kuhajda F.P. AMP-activated protein kinase and human cancer: cancer metabolism revisited. Int J Obes (Lond) 2008;32 Suppl 4:S36-S41.

Kuin A., Smets L., Volk T., Paans A., Adams G., Atema A., et al. Reduction of intratumoral pH by the mitochondrial inhibitor m-iodobenzylguanidine and moderate hyperglycemia. Cancer Res 1994;54(14):3785-92.

Laconi E. The evolving concept of tumor microenvironments. Bioessays 2007;29(8):738-44.

Loadman P.M., Bibby M.C., Phillips R.M. Pharmacological approach towards the development of indolequinone bioreductive drugs based on the clinically inactive agent EO9. Br J Pharmacol 2002;137(5):701-9.

Luciani F., Spada M., de M.A., Molinari A., Rivoltini L., Montinaro A., et al. Effect of proton pump inhibitor pretreatment on resistance of solid tumors to cytotoxic drugs. J Natl Cancer Inst 2004;96(22):1702-13.

Marsin A.S., Bertrand L., Rider M.H., Deprez J., Beauloye C., Vincent M.F., et al. Phosphorylation and activation of heart PFK-2 by AMPK has a role in the stimulation of glycolysis during ischaemia. Curr Biol 2000;10(20):1247-55.

Mathupala S.P., Colen C.B., Parajuli P., Sloan A.E. Lactate and malignant tumors: a therapeutic target at the end stage of glycolysis. J Bioenerg Biomembr 2007;39(1):73-7.

McKeown S.R., Cowen R.L., Williams K.J. Bioreductive drugs: from concept to clinic. Clin Oncol (R Coll Radiol) 2007;19(6):427-42.

McMahon G. VEGF receptor signaling in tumor angiogenesis. Oncologist 2000;5 Suppl 1:3-10.

Melino G., De L., V, Vousden K.H. p73: Friend or foe in tumorigenesis. Nat Rev Cancer 2002;2(8):605-15.

Minchenko A., Leshchinsky I., Opentanova I., Sang N., Srinivas V., Armstead V., et al. Hypoxia-inducible factor-1-mediated expression of the 6-phosphofructo-2-kinase/fructose-2,6-bisphosphatase-3 (PFKFB3) gene. Its possible role in the Warburg effect. J Biol Chem 2002;277(8):6183-7.

Nieder C., Wiedenmann N., Andratschke N., Molls M. Current status of angiogenesis inhibitors combined with radiation therapy. Cancer Treat Rev 2006;32(5):348-64.

nkova-Kostova A.T., Talalay P. NAD(P)H:quinone acceptor oxidoreductase 1 (NQO1), a multifunctional antioxidant enzyme and exceptionally versatile cytoprotector. Arch Biochem Biophys 2010.

Owen J.B., Coia L.R., Hanks G.E. Recent patterns of growth in radiation therapy facilities in the United States: a patterns of care study report. Int J Radiat Oncol Biol Phys 1992;24(5):983-6.

Park H., Lyons J.C., Griffin R.J., Lim B.U., Song C.W. Apoptosis and cell cycle progression in an acidic environment after irradiation. Radiat Res 2000;153(3):295-304.

Patterson L.H., Murray G.I. Tumour cytochrome P450 and drug activation. Curr Pharm Des 2002;8(15):1335-47.

Petrangolini G., Supino R., Pratesi G., Dal B.L., Tortoreto M., Croce A.C., et al. Effect of a novel vacuolar-H+-ATPase inhibitor on cell and tumor response to camptothecins. J Pharmacol Exp Ther 2006;318(3):939-46.

Poon E., Harris A.L., Ashcroft M. Targeting the hypoxia-inducible factor (HIF) pathway in cancer. Expert Rev Mol Med 2009;11:e26.

Pozuelo R.M., Peggie M., Wong B.H., Morrice N., MacKintosh C. 14-3-3s regulate fructose-2,6-bisphosphate levels by binding to PKB-phosphorylated cardiac fructose-2,6-bisphosphate kinase/phosphatase. EMBO J 2003;22(14):3514-23.

Raghunand N. Tissue pH measurement by magnetic resonance spectroscopy and imaging. Methods Mol Med 2006;124:347-64.

Raghunand N., Gillies R.J. pH and drug resistance in tumors. Drug Resist Updat 2000;3(1):39-47.

Rekwirowicz H., Marszalek A. Hypoxia-inducible factor-1, a new possible important factor in neoplasia. Pol J Pathol 2009;60(2):61-6.

Rouschop K.M., Wouters B.G. Regulation of autophagy through multiple independent hypoxic signaling pathways. Curr Mol Med 2009;9(4):417-24.

Rozhin J., Sameni M., Ziegler G., Sloane B.F. Pericellular pH affects distribution and secretion of cathepsin B in malignant cells. Cancer Res 1994;54(24):6517-25.

Seddon B., Kelland L.R., Workman P. Bioreductive prodrugs for cancer therapy. Methods Mol Med 2004;90:515-42.

Semenza G.L. Hypoxia and cancer. Cancer Metastasis Rev 2007;26(2):223-4.

Semenza G.L. Hypoxia-inducible factor 1 and cancer pathogenesis. IUBMB Life 2008a;60(9):591-7.

Semenza G.L. Regulation of cancer cell metabolism by hypoxia-inducible factor 1. Semin Cancer Biol 2009;19(1):12-6.

Semenza G.L. Tumor metabolism: cancer cells give and take lactate. J Clin Invest 2008b;118(12):3835-7.

Shi Q., Le X., Wang B., Abbruzzese J.L., Xiong Q., He Y., et al. Regulation of vascular endothelial growth factor expression by acidosis in human cancer cells. Oncogene 2001;20(28):3751-6.

Smallbone K., Gatenby R.A., Gillies R.J., Maini P.K., Gavaghan D.J. Metabolic changes during carcinogenesis: potential impact on invasiveness. J Theor Biol 2007;244(4):703-13.

Smallbone K., Gavaghan D.J., Gatenby R.A., Maini P.K. The role of acidity in solid tumour growth and invasion. J Theor Biol 2005;235(4):476-84.

Sollner S., Macheroux P. New roles of flavoproteins in molecular cell biology: an unexpected role for quinone reductases as regulators of proteasomal degradation. FEBS J 2009;276(16):4313-24.

Song C.W., Kang M.S., Rhee J.G., Levitt S.H. The effect of hyperthermia on vascular function, pH, and cell survival. Radiology 1980;137(3):795-803.

Spanswick V.J., Cummings J., Ritchie A.A., Smyth J.F. Pharmacological determinants of the antitumour activity of mitomycin C. Biochem Pharmacol 1998;56(11):1497-503.

Stratford I.J., Williams K.J., Cowen R.L., Jaffar M. Combining bioreductive drugs and radiation for the treatment of solid tumors. Semin Radiat Oncol 2003;13(1):42-52.

Thangasamy T., Sittadjody S., Lanza-Jacoby S., Wachsberger P.R., Limesand K.H., Burd R. Quercetin selectively inhibits bioreduction and enhances apoptosis in melanoma cells that overexpress tyrosinase. Nutr Cancer 2007;59(2):258-68.

Thoreen C.C., Sabatini D.M. AMPK and p53 help cells through lean times. Cell Metab 2005;1(5):287-8.

Thoreen C.C., Sabatini D.M. AMPK and p53 help cells through lean times. Cell Metab 2005;1(5):287-8.

Tong R.T., Boucher Y., Kozin S.V., Winkler F., Hicklin D.J., Jain R.K. Vascular normalization by vascular endothelial growth factor receptor 2 blockade induces a pressure gradient across the vasculature and improves drug penetration in tumors. Cancer Res 2004;64(11):3731-6.

Tozer G.M., Bicknell R. Therapeutic targeting of the tumor vasculature. Semin Radiat Oncol 2004;14(3):222-32.

Tsvetkov P., Reuven N., Shaul Y. Ubiquitin-independent p53 proteasomal degradation. Cell Death Differ 2010;17(1):103-8.

van Herwaarden A.E., Wagenaar E., Merino G., Jonker J.W., Rosing H., Beijnen J.H., et al. Multidrug transporter ABCG2/breast cancer resistance protein secretes riboflavin (vitamin B2) into milk. Mol Cell Biol 2007;27(4):1247-53.

Vaupel P., Mayer A. Hypoxia in cancer: significance and impact on clinical outcome. Cancer Metastasis Rev 2007;26(2):225-39.

Wachsberger P., Burd R., Dicker A.P. Improving tumor response to radiotherapy by targeting angiogenesis signaling pathways. Hematol Oncol Clin North Am 2004;18(5):1039-57, viii.

Wachsberger P.R., Burd R., Cardi C., Thakur M., Daskalakis C., Holash J., et al. VEGF Trap in combination with radiotherapy improves tumor control in U87 glioblastoma. Int J Radiat Oncol Biol Phys 2007.

Weyergang A., Berg K., Kaalhus O., Peng Q., Selbo P.K. Photodynamic therapy targets the mTOR signaling network in vitro and in vivo. Mol Pharm 2009;6(1):255-64.

Williams A.C., Collard T.J., Paraskeva C. An acidic environment leads to p53 dependent induction of apoptosis in human adenoma and carcinoma cell lines: implications for clonal selection during colorectal carcinogenesis. Oncogene 1999;18(21):3199-204.

Williams K.J., Cowen R.L., Brown L.M., Chinje E.C., Jaffar M., Stratford I.J. Hypoxia in tumors: molecular targets for anti-cancer therapeutics. Adv Enzyme Regul 2004;44:93-108.

Winkler F., Kozin S.V., Tong R.T., Chae S.S., Booth M.F., Garkavtsev I., et al. Kinetics of vascular normalization by VEGFR2 blockade governs brain tumor response to radiation: role of oxygenation, angiopoietin-1, and matrix metalloproteinases. Cancer Cell 2004;6(6):553-63.

ykin-Burns N., Ahmad I.M., Zhu Y., Oberley L.W., Spitz D.R. Increased levels of superoxide and H2O2 mediate the differential susceptibility of cancer cells versus normal cells to glucose deprivation. Biochem J 2009;418(1):29-37.

Yu J.L., Coomber B.L., Kerbel R.S. A paradigm for therapy-induced microenvironmental changes in solid tumors leading to drug resistance. Differentiation 2002;70(9-10):599-609.

Zhang J., Stevens M.F., Laughton C.A., Madhusudan S., Bradshaw T.D. Acquired Resistance to Temozolomide in Glioma Cell Lines: Molecular Mechanisms and Potential Translational Applications. Oncology 2010;78(2):103-14.

Zhuang W., Qin Z., Liang Z. The role of autophagy in sensitizing malignant glioma cells to radiation therapy. Acta Biochim Biophys Sin (Shanghai) 2009;41(5):341-51.